TD-03-008
Beamsdoc 480
03/03
rev1 01/05

ANALYSIS OF THE SEXTUPOLE CORRECTION IN THE TEVATRON

REVISION 1

G. Annala, G. Ambrosio, P. Bauer[1], J. DiMarco, R.W. Hanft, M.J. Lamm, M. Martens, P. Schlabach, M. Tartaglia, J.C. Tompkins, G. Velev

Fermilab

Beam loss and emittance dilution during ramping from injection to collision energy is observed in the Tevatron, now in its collider run-II stage. There is evidence indicating that this is mostly related to beam instabilities. There also is concern, however, that imperfect control of the machine chromaticity during the injection porch and the ensuing ramp to collision could contribute to or exacerbate the beam loss. It is well known that the magnetic multipoles and most importantly the sextupole component in the superconducting dipole magnets in the Tevatron decay during the injection plateau and snap back to the value before the start of the decay at the start of the ramp. Sextupole correctors distributed around the ring are used to counteract the sextupole decay and snapback in the main magnets. To determine if the sextupole compensation is working successfully in the Tevatron a thorough investigation of the Tevatron chromaticity settings and corrections was conducted. The amount of sextupole in the machine at injection and during the ramp was derived from beam chromaticity measurements and compared to the amount of sextupole expected on the basis of recently conducted (as well as archived) magnetic measurements performed on Tevatron dipole magnets. The following reports on the results of this comparison, showing that the sextupole decay and snapback compensation in the Tevatron can be improved. These improvements are discussed, as well as the sextupole compensation scheme currently used in the machine. This note was recently revised to include the latest results of an extensive study of sextupole drift and snapback in several Tevatron dipole magnets. These results, which were only partially available at the time of the first publication of this note, have allowed to strengthen the case for improvements of the Tevatron sextupole correction scheme.

[1] e-mail: pbauer@fnal.gov

TABLE OF CONTENT

1) Dynamic Effects in Superconducting Magnets 3
2) Sextupole Decay and Snapback Correction in the Tevatron 4
3) Comparison of Tevatron Decay & Snapback Fit and Magnet Data 6
4) Beam Based b2 Measurements in the Tevatron 12
5) Comparison of Beam and Magnet Based b2 Measurements 17
6) Conclusions and Recommendations 21
APPENDIX 1 29
APPENDIX 2 31
APPENDIX 3 32
APPENDIX 4 36
APPENDIX 5 37
APPENDIX 6 39

1) Dynamic Effects in Superconducting Magnets

It is well known that the magnetic multipoles and most importantly the sextupole (b_2) component in the superconducting dipole magnets in the Tevatron decay by approximately 1-2 units (defined as 10^{-4} of the main dipole field in the bore and measured at the reference radius of 25.4 mm) during the injection plateau, [1]. During the first few seconds of the ramp from the injection porch the b_2 quickly snaps back to the initial level before the decay while at the same time evolving along the hysteretic loop. These effects were first discovered in the Tevatron and are referred to as dynamic effects. Figure 1 shows the hysteretic sextupole loop in a Tevatron dipole magnet (TC0504). The zoom-in portion shows the drift and snapback during and after a 15 min dwell at the injection current. The figure clearly shows how the hysteretic b_2 evolves around the so-called geometric b_2. The geometric b_2 in the example of Figure 1 is 13 units, which is typical for the Tevatron dipole magnet body, [2]. As shown in the zoom-in region the b_2 drifts toward the geometric during the injection porch and snaps back to the hysteretic loop as the ramp starts.

Qualitative models exist that help explain the dynamic effects observed in superconducting magnets, [3], with slow changes of the current distribution between the strands in the multi-stranded cable from which the coils are wound. A non-uniform inter-strand current distribution produces sinusoidal field variations along the cable with a period equal to the twist pitch of the strands in the cable. The current imbalances, caused for example by varying splice to strand resistances or spatially varying *dB/dt* in the magnet ends, vary only slowly with time (time constants of thousands of seconds) because the currents are running for the most part in zero resistance superconductor. The time constant(s) also strongly depend(s) on the distribution of (cross and adjacent) contact resistances along the cable in the coils. The drift effects found in the magnetic multipoles are the result of a demagnetization of the superconducting filaments due to the

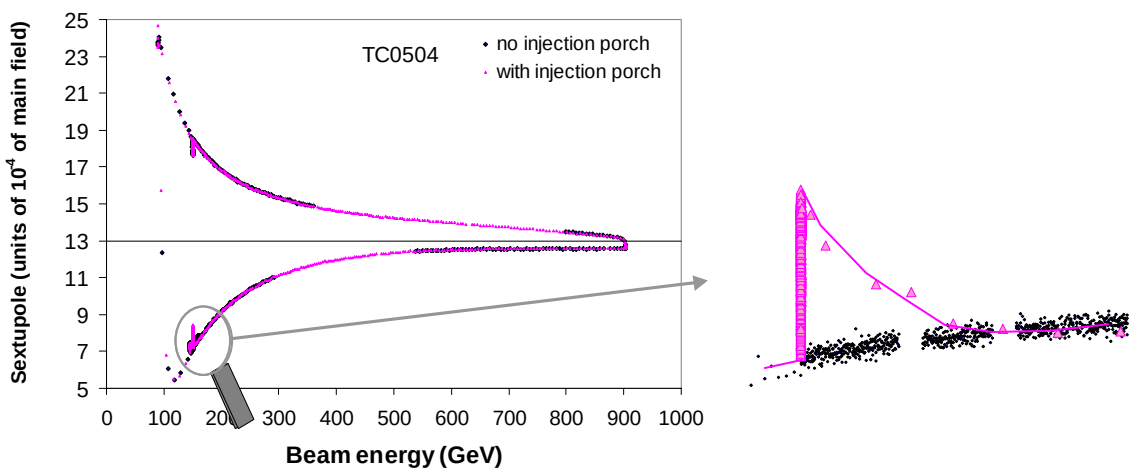

Figure 1: Example of b_2 (at 25.4 mm radius) drift and snapback in Tevatron model TC0504. The right plot is a blow-up of the drift and snapback during and after injection. For comparative purposes measurements with and without dwell at injection are shown.

local field variations in the strands when the currents redistribute between strands. During ramping of the magnet the local field changes due to current redistribution are smaller than the field change due to the ramp and thus the demagnetization effects are suppressed. At constant excitation such at injection, however, a de-magnetization of the strands occurs producing the dynamic behavior of the sextupole seen in Figure 1. The dynamic effects depend on the ramping history of the magnet because the sequence, type and direction of ramps and fixed field dwells strongly influence the amplitude and pattern of the inter-strand current distribution.

2) Sextupole Decay and Snapback Correction in the Tevatron

The sextupole drift and snapback in Tevatron magnets are corrected using two sextupole corrector circuits C:SFB2 and C:SDB2 (in the Tevatron notation), which control 176 sextupole correctors around the ring. Note that the b_2 correction scheme described here compensates only for the dynamic (drift and snapback) b_2 component in the magnets. It plays out on top of the correction of the hysteretic and geometric b_2 in the dipole magnets (T:SF and T:SD). The currently used dynamic b_2 compensation is derived from fits of the b_2 decay and snapback characteristics measured in 1996 on one Tevatron dipole, TC1052 [4]. These fits are functions of different pre-cycle parameters, such as the flat-top time and back-porch time. The following describes the currently installed dynamic b_2 correction algorithm, which is based on these fits. A description of the b_2 correction algorithm can also be found in [5]. The fits also reflect characteristics of the drift and snapback patterns in Tevatron magnets found in earlier measurement campaigns (see for example reference [6] for further details regarding these earlier magnet studies). Note that there is a slight disagreement between the fits used now in the Tevatron and presented here or in [5] and those derived directly from the magnet tests [4]. This difference, in the coefficients but not in form, reflects beam-based adjustments of the original algorithm in the Tevatron. These adjustments were to be expected because the characteristics of the dynamic effects scatter considerably between different magnets and it is therefore unlikely that one magnet is representative of the all-magnet average that determines the behavior of the Tevatron. A quantitative estimate of the beam-based adjustments is given in appendix 3. Also note that the parameters of the algorithm depend not only on the durations of the various constant field dwells in the pre-cycle but also on the accelerator powering waveform, which is assumed to be the current collider run-II waveform. *Schematic 1* shows the basic layout of the Tevatron waveform, including the pre-cycle. The injection current is 666 A (0.660 T dipole field, 150 GeV beam energy) and the flat-top current is 4333 A (4.330 T, 980 GeV). The magnetization reset is performed at 90 GeV. The pre-cycle primarily serves to stabilize the magnetic field quality of the magnets at injection, since, especially at low fields, the multipole content in the magnets during the virgin cycles differs from that in subsequent cycles. Given the powering history dependence of dynamic effects, the pre-cycle also serves to bring all magnets into a more homogeneous magnetic state in terms of their dynamic effects.

The fit of the sextupole decay at injection (in units of the main dipole at 25.4 mm), on the basis of which the sextupole corrector currents in Tevatron run II are derived, as a

function of back-porch t_{bp}, flat-top time t_{ft} and time at the injection porch (all in seconds) is given in equation (1).

$$b_2^{drift}\left(t_{bp}, t_{ft}, t\right) = b_2^{ini}\left(t_{bp}, t_{ft}\right) + m\left(t_{bp}, t_{ft}\right)\ln(t) \quad units\ at\ 1'', \tag{1}$$

where the initial sextupole (in units at 25.4 mm) at injection (the so-called intercept) before the start of the decay is given with:

$$b_2^{ini}\left(t_{bp}, t_{ft}\right) = -A\ln\left(\frac{t_{bp}}{60}\right) - \left[B - C\ln\left(\frac{t_{bp}}{60}\right)\right]\ln\left(t_{bp}\right) \quad units\ at\ 1''\ . \tag{2}$$

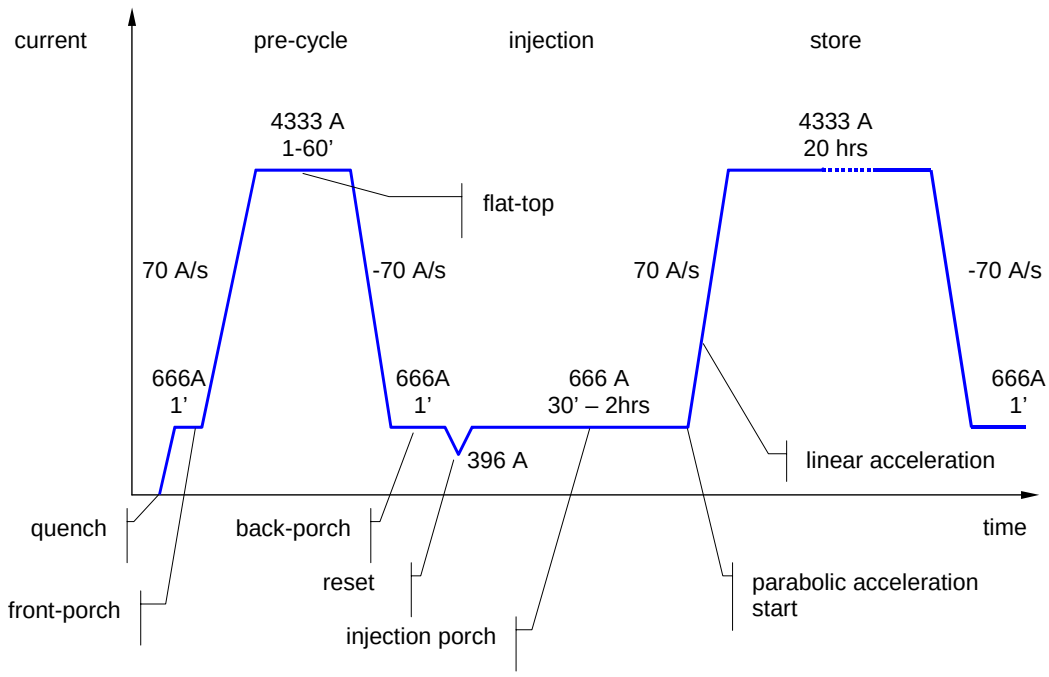

Schematic 1: Tevatron ramp-cycle including pre-cycle, injection porch and ramp to collision. Note that in most cases the store is followed by a pre-cycle and therefore the zero-field condition is rare. Also in case of a quench in the Tevatron and ramping from zero a sequence of six 1 min flat-top pre-cycles is performed rather than only one as indicated here.

The scaling constant m (the slope of the decay in units/decade) as a function of back-porch and flat-top time is:

$$m\left(t_{bp}, t_{ft}\right) = D - E \cdot \left[2\ln\left(t_{bp}\right) - \ln\left(t_{ft}\right)\right]. \tag{3}$$

The parameters of the intercept and slope fits, (2) and (3), are listed in Table 1.

Table 1: Parameters of sextupole decay algorithm presently used in the Tevatron, equ. (2) & (3).

Parameter	A	B	C	D	E
Tevatron	0.04	0.161	0.0277	0.342	0.0208

The snapback compensation (as a function of the snapback duration t_{sb}) is:

$$b_2^{snap}\left(t_{bp}, t_{ft}, t_{inj}, t_{sb}, t\right) = b_2^{drift}\left(t_{bp}, t_{ft}, t_{inj}\right)\left[1-\left(\frac{t}{t_{sb}}\right)^2\right]^2 \quad units\ at\ 1'', \tag{4}$$

where $b_2^{drift}(t_{bp},t_{ft},t_{inj})$ is the sextupole (in units) at the end of the injection porch (at $t=t_{inj}$), as calculated from the decay fit (1) and t_{sb} is the duration of the snapback (which is currently programmed to be 6 sec in the Tevatron).

A total of 176 sextupole correctors, in two families (SD, SF) alternating around the ring, are injected with a current to compensate the sextupole decay and snapback at the start of the ramp. The SF/SD units are located next to the horizontally/ vertically focusing quadrupoles (where β_x/β_y is large), therefore having a large effect on the horizontal/vertical chromaticity. Equations (5) and (6) are used in TCHROM to convert the b_2 algorithm into current in the sextupole correctors to compensate for the b_2 in the dipoles. The coefficients were measured a long time ago in the Tevatron. Appendix 1 gives a theoretical derivation of (5) and (6). There is a discrepancy between the calculated coefficients in appendix 1 and the measured coefficients in (5) and (6). Also, recent measurements of the coefficients in (5) and (6) have given results that are closer to the calculated values. The variation of these parameters with time is not well understood. The difference between the "real" parameters and those in TCHROM necessitates either their modification or an adaptation of the b_2 algorithm to achieve successful b_2 compensation.

$$I_{T:SFB2}(t) = -0.4964\, b_2(units) \quad (A) \tag{5}$$

$$I_{T:SDB2}(t) = -0.765\, b_2(units) \quad (A) \tag{6}$$

3) Comparison of Tevatron Decay & Snapback Fit and Magnet Data

Figure 2 compares the b_2 calculated with (1)-(4) with the sextupole decay and snapback measured on magnet TC1052 in 1996 [4] for a 1 min back-porch and a 10 min flat-top pre-cycle. The fit agrees well with the magnetic measurement (except for the drift at t<5 min, see discussion below). This is in part expected, given that the Tevatron fit is based on TC1052 data, and in part surprising because the fit parameters in Table 1 are not exactly those obtained from the measurement on magnet TC1052, but include further refinements implemented during commissioning of Tevatron run II. The refinements of the fit were needed to –1- adapt the fit from dipole (1052) to the "average" Tevatron dipole, -2- to address differences in key operational parameters between the test of 1052 and the Tevatron, such as for example in the pre-cycle flat-top energy (980 GeV in the Tevatron and 900 GeV in the magnet test) and the operational temperature of the magnets (~4 K in the Tevatron and ~4.5 K in the magnet test). These refinements, which were implemented during run II commissioning, are discussed in appendix 3. Let me repeat,

however, that, in general, agreement between the Tevatron b_2-fit and the b_2 measured in a particular magnet is not expected. This Tevatron fit should represent the average of all dipole magnets installed in the ring. Therefore, and given the considerable magnet-to-magnet spread in the hysteretic as well as the dynamic b_2 characteristics, such an agreement would be fortuitous coincidence. As discussed in further detail in [8] the magnet-to-magnet spread of for instance the drift amplitude for a given pre-cycle is ~100 %. As far as can be judged on the basis of measurements in 1% of the magnets (see [8]) magnet TC1052 is average in terms of its drift amplitude. Comparisons such as in Figure 2 were also performed for other pre-cycle parameter combinations. Some of the resulting plots are shown in appendix 2 (Figure 17 and Figure 18) and they show that the agreement is not always as good as in Figure 2.

The magnetic measurement data in Figure 2 were offset corrected, i.e. the geometric (13 units) and the hysteretic magnetization (-4.5 units) b_2 at 150 GeV were subtracted from the data, such as to show the decay and snapback only. Also the change of hysteretic b_2 during the snapback was removed (in TC1052 the b_2-hysteresis loop is approximately linear with $k_{b2}=0.00935$ *units/A*). No temperature correction was applied, although there is a discrepancy between the average magnet temperature in the Tevatron (currently ~4 K, [9]) and the temperature at which the measurement on TC1052 was performed (~4.5 K). Furthermore, the fit parameters were derived on the basis of measurements with a 900 GeV flat-top energy in the pre-cycle, while the pre-cycle flat-top in the Tevatron today is 980 GeV. The effect of the pre-cycle flat-top energy on the drift and snapback is more or less known from measurements on magnets, [4,8]. If one would include a correction of the magnet measurement data for the discrepancy in pre-cycle flat-top energy (also see discussion in appendix 3) a larger discrepancy between the fit and the TC1052 data would appear in Figure 2. The differences in operational temperature and pre-cycle parameters are two additional facts that make the agreement found in Figure 2 appear even more as a fortuitous coincidence.

Figure 2 shows a significant discrepancy between fit and magnet data at times smaller than one minute. This is the result of an offset of ~(-1) unit in the calculated b_2 that allows for a good fit of the data at $t>1$ *min* using the simple logarithmic function (equ. (1)). Extensive b_2 measurements on a dozen Tevatron spare dipoles (discussed in [8]) indicate that a more complicated function than equation (1) is required to fit the drift at all times. One option for instance, uses an exponential function with two time constants, one for $t<1min$ and another for $t>1min$. Another option, which was suggested in [4], but not implemented in the Tevatron, is to introduce an offset in the log-function argument. We are also proposing a new fit function at the end of this note (section 6). It is noteworthy that the discrepancy at small times does not affect the Tevatron operation because: -1- the beam is never injected before several minutes on injection porch, -2- the current table for the sextupole correction (C:SFB2 and C:SDB2) automatically sets the current to zero at $t=0$ (where the logarithmic function diverges). The current at the next time point in the current table is computed from the b_2 algorithm ((1)-(4)) and the corrector current – b_2 conversion ((5)-(6)) at 1.667 min. The correction currents fed into the SF and SD sextupole correctors (which are calculated from the b_2 fit) are shown in Figure 3 together with currents extracted from the Tevatron tables for a particular run

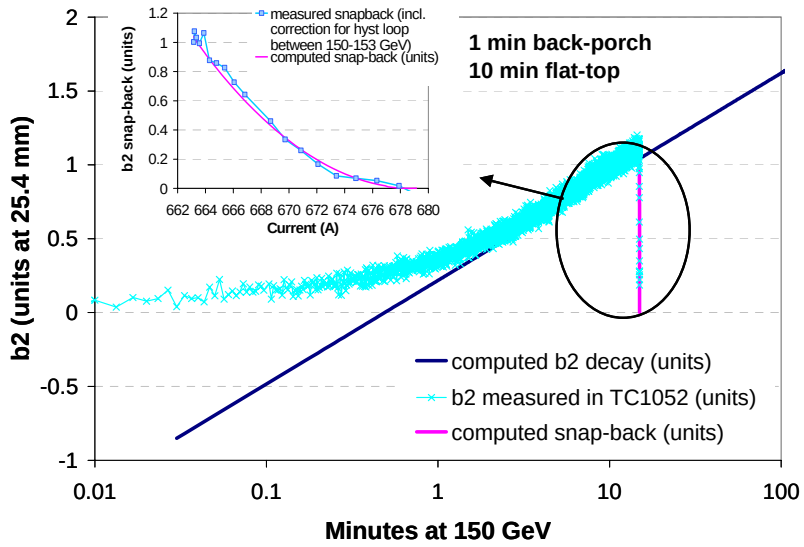

Figure 2: Comparison of decay compensation algorithm for Tevatron injection (equ. 1&4, Table 1) and magnetic measurements on TC1052 reported in [4]. Measurements on TC1052 were performed with a 10 min flat-top and 1 min back-porch (2 pre-cycles). The fit was calculated for similar pre-cycle parameters. Note that the pre-cycle flattop energy was 900 GeV in the magnet measurement and is assumed to be 980 GeV in the Tevatron (there is no pre-cycle flat-top energy parameter in the fit). The insert shows a zoom into the snapback region. The snapback is plotted as a function of current. The hysteretic baseline of the snapback was removed.

(Tev run 1776). The calculated and measured data compare reasonably well. As indicated above the calculated currents do not follow a straight line as expected from (1)-(3) and

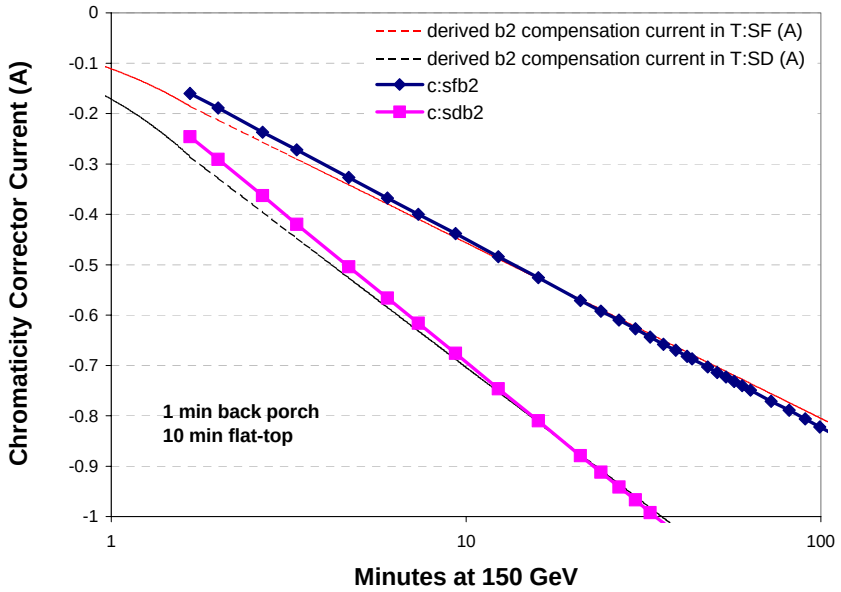

Figure 3: Sextupole currents calculated from equations (1)-(6) and as used in the Tevatron (on the basis of the same fit). C:SFB2 and C:SDB2 settings were taken for Tevatron run 1766 (Sept. 18th 2002).

(5)-(6) because they are set to zero at *t=0* and interpolated linearly between zero and the current computed at the first time point at *t=1.667 min*.

More important than the compensation of the drift, however, is the correction for the fast snapback. An extensive measurement campaign conducted recently to improve the understanding of dynamic effects in Tevatron dipole magnets (and reported in [8]) has revealed the following characteristics. The drift amplitudes for a given pre-cycle vary by up to a factor two between different dipole magnets. Figure 4 shows a collection of snapbacks after a 30 min dwell at injection (and following a pre-cycle with 1 min front-porch, 20 min flat-top and 1 min back-porch) measured in eight Tevatron dipoles. The plot clearly shows the spread in drift amplitudes. The plot in Figure 4 also shows that the Tevatron snapback algorithm predicts a shorter snapback than those measured. This is related to the fact that the snapback fit (equ. 4) was modeled after the 1996 magnetic measurement data. These data were recorded after a 15 min dwell at injection, thus after less drift than occurred during the 30 min injection dwell shown in Figure 4. It is now known that the snapback duration depends on the amount of drift that occurred before the start of the snapback, [13]. Longer dwells at injection and particular pre-cycle parameter combinations such as short back-porch times result in even larger drift amplitudes than those shown in Figure 4. The currently used fit algorithm does not adapt to the varying snapback durations since it consists of a function that becomes zero at the so-called snapback time (currently 6 secs). There is a reason, however, why this shortcoming is partially mitigated in the Tevatron. Theory and experiment indicate that the correlation underlying the correlation between snapback duration and drift amplitude is a correlation between the drift amplitude and the amount of bore-field needed to resolve the snapback

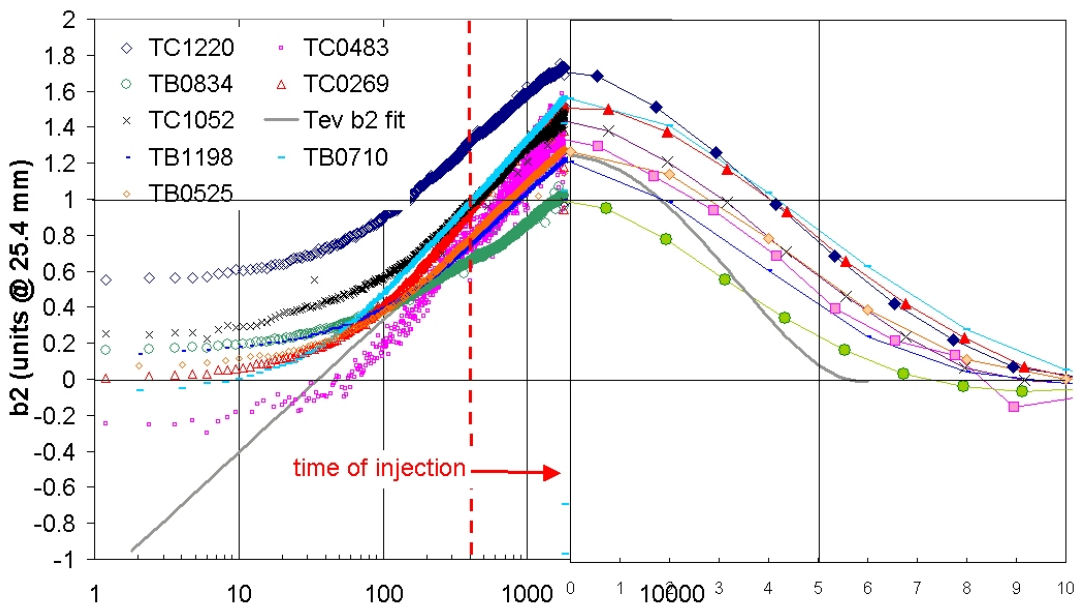

Figure 4: Comparison of snapbacks measured on eight Tevatron magnets during the 2003 *b2* measurement campaign and the calculated snapback based on the Tevatron snapback fit (equ. 4). The hysteretic and geometric *b2* was removed from the magnet data such as to show the dynamic *b2* only. The measurements are reported in detail in [8].

and re-magnetize the coils. Since the magnetic field grows with the square of time on the (parabolic) ramp, the durations of the snapbacks are compressed, i.e. snapback from large drifts do not take much longer than from small drifts. Figure 4 in fact shows that compression effect in the snapbacks measured on several magnets. Snapbacks that start from twice the drift amplitude don't take twice as long as they would on a linear ramp.

The main conclusion to be drawn from Figure 4, however, is that the snapback fit currently used in the Tevatron clearly underestimates the snapback duration in the Tevatron. The snapback time in the Tevatron algorithm (equ. 4) was derived on the basis of the snapbacks measured in TC1052 and TC0504, which appear to be shorter than what is measured in the magnets today. Some of these measurements are shown in Figure 5. Figure 5 shows that the snapback duration following a one unit drift is close to ~4 sec. This is related to the fact that the magnetic measurements were performed with the Tevatron collider run I ramp, which was steeper than the ramp used today. Figure 25 in appendix 4 shows the difference between the run I and run II current ramp profiles during the initial (snapback) part of the ramp. This effect was taken into account when defining the snapback time for run II (6 secs). It appears, however, that the much longer injection porch duration in Tevatron operation today (~2 hrs) was not taken into account when the snapback time was adapted to the run II conditions. Therefore the currently chosen snapback time falls short of what is expected to occur in the Tevatron (based on the results of recent measurements in magnets, as presented above and reported in [8]).

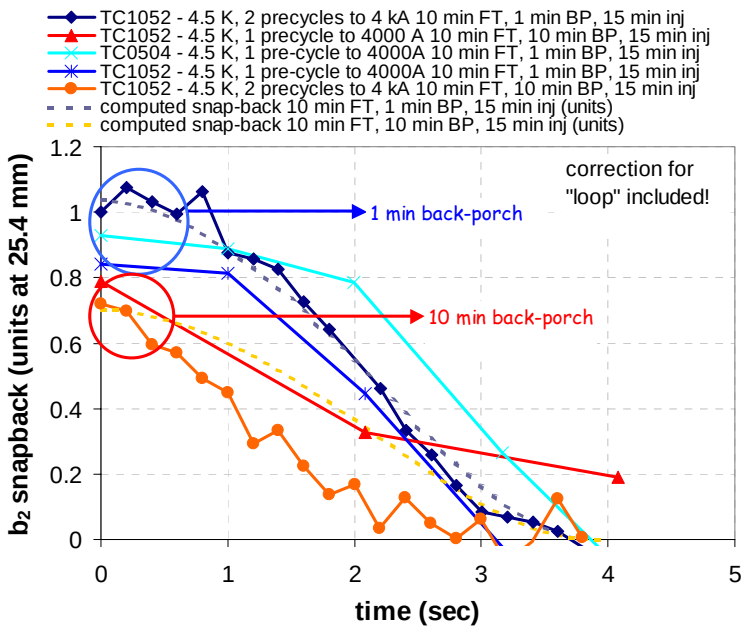

Figure 5: Comparison of snapbacks measured on TC1052 and TC0504 and the calculated snapback based on the Tevatron snapback fit (equ. 4) after 15 mins on the injection porch following pre-cycles with different back-porch durations. Note that the magnetic measurements were performed with the Tev96 ramp, resulting in faster snapbacks. A 4 secs snapback time was used in the fits. Also the magnet data are corrected for the increase in hysteretic b_2 during the snapback. The Tevatron 96 ramp is shown together with the current Tevatron ramp in Figure 25 in appendix 4.

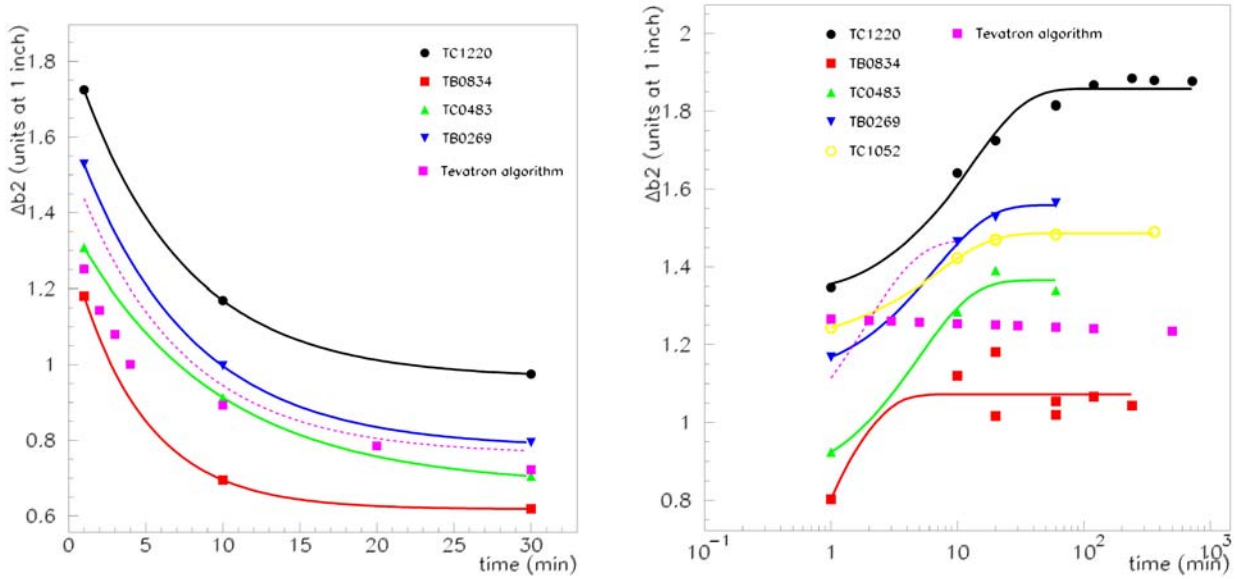

Figure 6: *b2* drift amplitude after 30 min at injection for different pre-cycle back-porch (left) and flat-top (right) durations in various Tevatron dipole magnets at 4.0 K. When not explicitly varied, the pre-cycle parameters were: 1 min front-porch, 20 min flat-top and 1 min back-porch. See [8] for further details on the measurements. Also shown is the *b2* drift amplitude calculated with the algorithm used currently for the *b2*-drift correction in the Tevatron (equ. 1-3).

The report on the b_2 measurements, [8], discusses in detail the dependence of drift and snapback on the powering history of the magnets. The recent measurements in MTF have confirmed one of the conclusions of the 96 campaign, namely that the most important parameters for the dynamic effects in Tevatron dipole magnets are the pre-cycle back-porch and flat-top durations (this obviously assumes that the only parameters varied in the Tevatron wave-form are the durations of the different porches). Figure 6 shows that the drift is more pronounced the shorter the dwell at the back-porch and the longer the dwell at flat-top. The back-porch duration is the pre-cycle parameter with the strongest effect. The second most important parameter is the flat-top duration, with increasing drift amplitude the longer the flat-top. Both the effects of the back-porch and flat-top duration saturate (Figure 6). This saturation is interpreted as evidence that the "memory" of the magnets appears to be ~40 mins. In order to have all magnets in a similar state (with the same "memory") it is necessary to ramp the machine through a ~40 min or longer beam-less pre-cycle. [8] also that the front-porch duration does not affect the drift amplitude (keeping the other parameters at: 20 min flat-top, 1 min back-porch). As will be discussed in chapter 6 the knowledge of how the pre-cycle parameters affect the drift characteristics can be translated into proposals for improvements of the Tevatron drift and snapback correction schemes.

Also shown in Figure 6 is that the dynamic b_2 fit currently used in the Tevatron only poorly agrees with the magnet data in terms of its dependence on the pre-cycle parameters. This is in part related to the fact that the parameter space was not sufficiently explored in the 1996 magnet measurements on which the fit is based, therefore limiting

the "mathematical" quality of the fit itself. Secondly, in particular in what refers to the effect of the flat-top time, it is the result of the retro-active change of some of the parameters (see appendix 3 for details) of the original fit during fine tuning of the fit in the Tevatron. The fine tuning perturbed the fit, such that it does not represent anymore the correct dependence found in the original magnet data. A more detailed discussion of possible improvements to the multi-parameter algorithm for the b_2 drift and snapback in the Tevatron dipoles will be given in chapter 6. It is also important to include the results of beam-based measurements in the Tevatron in this discussion. The beam-based b_2 measurements in the Tevatron will be discussed next.

4) Beam Based b2 Measurements in the Tevatron

The preceding chapters discussed the comparison of the b_2 decay and snapback correction in the Tevatron with results from measurements performed on selected magnets. Some shortcomings of the correction algorithm were found. This chapter discusses recent indirect measurements of the average b_2 of *all* Tevatron magnets, derived from measurements of the beam chromaticity. Only these measurements can reveal what the average b_2 in the machine is. Beam chromaticity measurements have been performed many times before, especially during the injection porch, in order to check the Tevatron b_2 drift compensation scheme. These measurements usually indicated that the chromaticity was within 1-2 units of the set-point. This means that the magnet b_2 was compensated with a precision of ~0.1 units, since 1 unit of uncompensated sextupole in all Tevatron dipoles results in ~25 units of horizontal chromaticity. Measurements of the chromaticity during the snapback and on the hysteretic loop (during the ramp to flat-top), however, have not been conducted before run II.

In the context of the recent effort to improve the luminosity performance of the Tevatron, a beam chromaticity study program was launched, aiming to improve the understanding of the chromaticity in the Tevatron during the injection porch and the ramp, with particular emphasis of the snapback during the first few seconds on the ramp. These measurements are documented in [7] and [12]. The chromaticity measurements were always performed with an un-coalesced protons-only beam on the center orbit. As for a regular shot the Tevatron was prepared with a beam-less pre-cycle, usually with a ~20 min flat-top ("dry squeeze"). After injecting the beam the tunes were measured as a function of time during the injection porch as well as up the ramp. On the injection porch the chromaticity drift is slow enough to allow for a complete chromaticity measurement (which takes ~1 min) involving a variation of the orbits via variations in the RF frequency. For the measurement of the chromaticity on the ramp, a complete ramp-cycle including the beam-less pre-cycle was performed for different RF frequency settings (-20, 0, +20 Hz from nominal). The derivative of the tunes as a function of RF frequency was interpreted as the instantaneous chromaticity.

The machine chromaticity can be used to derive the average b_2 of all the magnets in the ring. Note that chromaticity and b_2 measurements on the ramp do not only reveal the dynamic b_2 (drift and snapback) of the Tevatron magnets but also the more conventional

hysteretic (and residual geometric) b_2 component(s). A detailed description of these components can be found in the summary note describing the recent magnet b_2 measurements, [8]. The derivation of the magnet b_2 from the chromaticity assumes that the measured chromaticity is the sum of the natural chromaticity (ξ_{nat}), the b_2 in the dipole magnets (ξ_{b2mag}) and the (compensating) b_2 supplied by the sextupole correctors (ξ_{b2corr}), such as stated in equation (7). Then, according to (7) the magnet b_2 is the measured chromaticity minus the natural and corrector-supplied chromaticity (note that there is an implicit negative sign in this contribution since it is supposed to compensate the b_2s in the magnets). The natural chromaticity as obtained from a Tevatron lattice model in MAD is –29.58 units of horizontal and –28.95 units of vertical chromaticity. The b_2 supplied by the sextupole correctors was derived from the sextupole correction currents extracted from the Tevatron control program together with the measured current to chromaticity conversion matrix such as in equations (A1) & (A2) from appendix 1. Note that the sextupole corrector term in equ. (7), ξ_{b2corr}, includes both the correction for the "static" (= geometric and hysteretic b_2 in magnets as well as natural and set-point) as well as the dynamic b_2, which are in fact provided by two different "cards" as described in section 2. The chromaticity related to the magnet b_2 as derived from equation (7) can then be converted to the b_2 with equation (A2) in appendix 1. A more detailed discussion of this procedure can be found in [12].

$$\xi_{tot} = \xi_{nat} + \xi_{b2mag} + \xi_{b2corr} \tag{7}$$

An example of the result of such a measurement is shown in Figure 7, indicating significant variations of the chromaticity on the ramp. Figure 8 shows the b_2 derived from the chromaticity measurements on a Tevatron injection porch ramp during Sept. 2002. The average magnet b_2 was inferred from the measured chromaticity according to the procedure described above. Figure 8 also shows a measurement of the b_2 on the injection porch in magnet TC0504 (data from the 1996 measurements). The agreement between magnet data and the b_2's derived from the Tevatron chromaticity is good. Note that the magnet b_2 data were offset corrected to fit the beam-based data. The offset correction procedure consists in subtracting the geometric sextupole of TC0504 (13.1 units) and adding a b_2 of 1.5 units. This step essentially replaces the geometric b_2 in the body of dipole 504 by the total average geometric b_2 in the Tevatron, which as discussed in another note, [8], is ~1.5 units according to the Tevatron magnetic measurement archive. The agreement of the drift characteristics measured in the Tevatron and in the TC0504 magnet is remarkable, indicating that the dynamic behavior of TC0504 is similar to that of the average Tevatron dipole. Note, however, that the injection porch in the magnetic measurement lasted only 15 min vs. more than 171 min in the beam based measurement and that the possibility of a divergence of the drifts after a longer injection porch cannot be excluded. Also, the exact pre-cycle parameter in the beam-based measurement was not recorded. (It was most likely a standard pre-cycle, which is characterized by a 1 min front-porch, 20 min flat-top and a 1 min back-porch.) Therefore Figure 8 provides a first impression of the precision of the b_2 drift correction, but experiments with better control of the pre-cycle parameters were performed later. These are reported next.

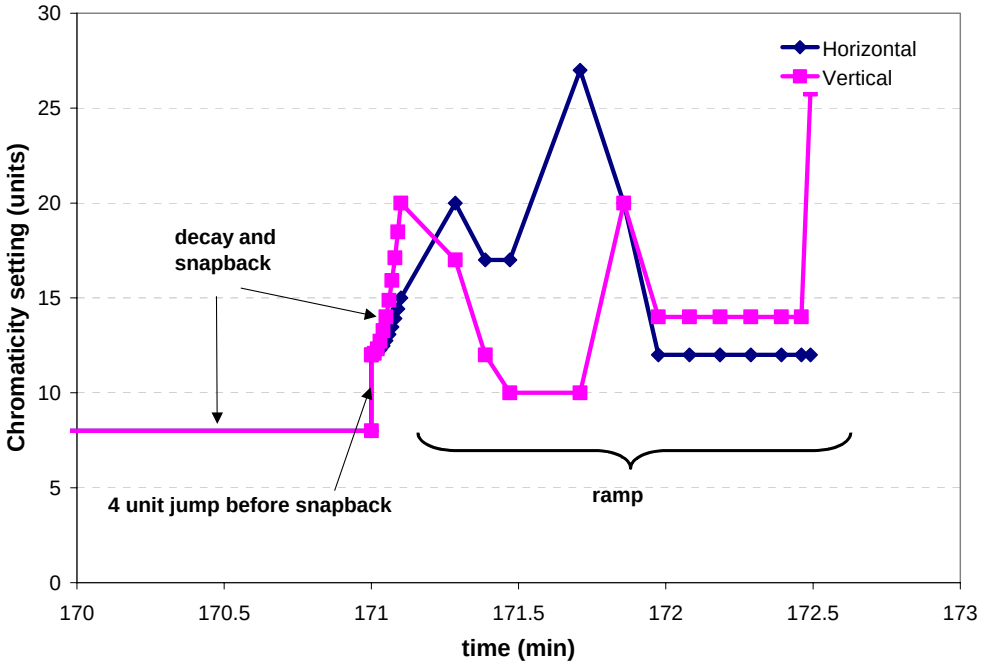

Figure 7: Tevatron chromaticity measured during Sept. 18th 2002 run.

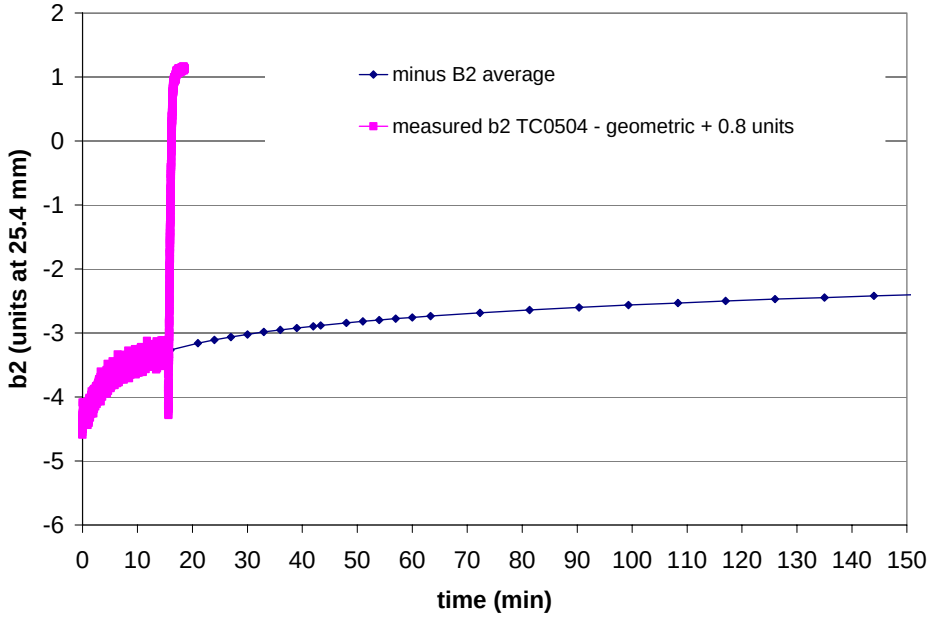

Figure 8: Sextupole as measured in TC0504 (without geometric sextupole) on Sept. 18th 2002 compared to b_2 derived from compensation currents in Tevatron control system.

Figure 9 shows the several beam-based b_2 measurements during the ramp recorded over two years. One of these cases consists only of a measurement at flat-top [10]. The pre-cycle conditions are unknown for the flat-top chromaticity measurement. This shouldn't matter, however, since the drift at flat-top is negligible. The other measurements are over part of the ramp and also comprise a snapback. The snapback starts from different drift-amplitudes because of the differences in injection porch duration. The smallest snapback occurred after a 6 sec injection porch (04/27/2004 data), the largest after a 171 min dwell on injection (09/18/2002 data). The latter data belong to the same set as that shown in Figure 8. As stated before, the exact pre-cycle parameters are unknown for this particular beam study. Also, being the first of its kind the confidence level in this data-set is the lowest of all shown. The Dec 4th data were recorded for a 20 min flat-top and 1 min back-porch pre-cycle. The 08/10/2004 data were recorded for a 1 hr flat-top and a 5 min back-porch pre-cycle and the 04/27/2004 data were recorded for a 12 sec flat-top and a 6 sec back-porch pre-cycle (Tevatron in the "ramping state").One can immediately recognize that these data appear to confirm the predicted correlation between drift amplitude and snapback duration, such as discussed in section 3 and [13]. This, despite the compression of the snapback on the ramp, which masks the effect when plotting the b_2 snapback versus time (see section 3 for more).

As discussed in further detail in the beam-study report ([7], [12]), the difference of the b_2 derived from the measured horizontal and vertical chromaticities is ~0.1 units (it is always the average of the two measurements that is shown in Figure 9). This difference, which is indicative of the measurement uncertainty, corresponds to an uncertainty of ~2 units of chromaticity. There is some uncertainty in the data, however, related to the data reduction procedure (as outlined above). One possible source of error could be related to the fact that the current-to-chromaticity coefficients are not well known for a particular measurement cycle. This matrix is a crucial component of the conversion of chromaticity data to b_2 data (see equation 7). Appendix 1 discusses the formulas used to derive the b_2 from the chromaticity, indicating that the calculated parameters (A6&A7) differ from the measured parameters (5&6) by up to 15%. This difference is unexplained and the measured coefficients were usually used in the analysis of the data. Also, the chromaticity measurement on the ramp takes at least three similar cycles (including the pre-cycle). This operation takes several hours (or can in some instances be spread over several days or weeks), during which some machine parameters, that also affect chromaticity, could change. For instance, a change in temperature in the magnets, from one cycle to the next by ~1 K could explain a chromaticity variation of this magnitude due to a ~15% change of hysteretic b_2 width in the magnets. (Such large temperature variations, however, are not believed to take place.)

Figure 10 shows a zoom into the snapback region for the beam based b2 measurements conducted on 08/10/2004 and 04/27/2004. The particularity of the 04/27/2004 measurement was that it was conducted with the Tevatron in the ramping state, i.e. with a minimum waiting time of 6 secs on the injection porch. Unexpectedly the data indicate a ~0.2 units snapback. This observation has triggered a new study of fast b_2 drifts in the Tevatron dipole magnets. This issue will briefly be touched upon again in chapter 6. A more detailed discussion can also be found in the corresponding beam study report [12].

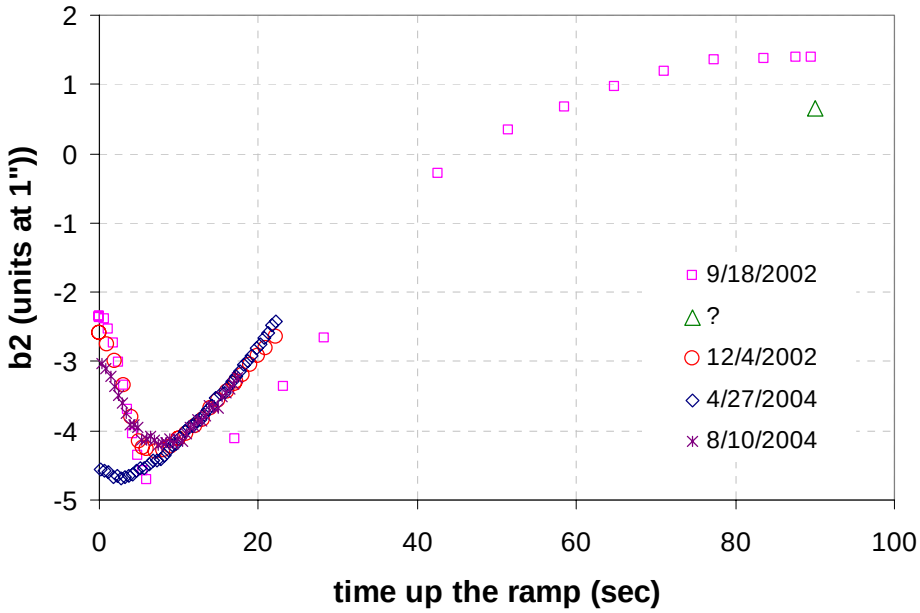

Figure 9: Beam based measurements of b_2 in the Tevatron, data are from [7,10,12]. The snapbacks shown occurred after 171 min (09/18/2002), 120 min (12/04/2002), 60 min (08/10/2004) and 6 sec (04/27/2004) on the injection porch. Also the pre-cycle conditions were different in all cases.

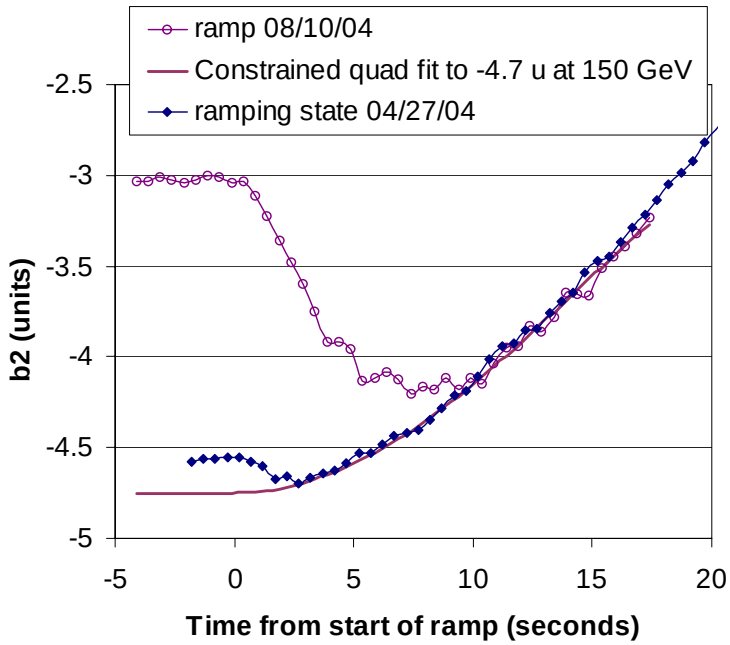

Figure 10: *b2* on the ramp in the Tevatron during the first 20 sec of the ramp as measured on 04/27/04 and 08/10/04. The solid line is the quadratic, constrained fit to the ramp *b2* measured on 08/10/04 using only the data from 160 GeV to 180 GeV in the fitting and constraining the t=0 value to –4.75 units.

5) Comparison of Beam and Magnet Based b2 Measurements

To investigate the quality of the b_2 compensation scheme in the Tevatron the beam-based b_2 measurements up the ramp discussed in chapter 5 have to be compared to the total, average b_2 in the Tevatron magnets as found from b_2 measurements in these magnets. Following magnet production in the 1980s magnetic measurements were performed in all Tevatron dipole magnets. Data for all the multipoles including b_2 across the entire length of each magnet as measured at the Fermilab Magnet Test Facility (MTF) are stored in a data archive. Also included were measurements at several currents, allowing reconstruction of the hysteretic loops for all multipoles. Unfortunately, dynamic effects were not known at that time and therefore not recorded. Dynamic effects in Tevatron magnets are known only from dedicated measurement campaigns conducted on a small number of magnets after commissioning of the Tevatron. The latest Tevatron dipole measurement campaign, [8], provides us with snapbacks for a dozen magnets, which is too little to produces a statistically significant average that is representative of the entire machine. But the issue is not only a lack of knowledge regarding the dynamic effects in the magnets. The Tevatron magnetic measurement archive does not only lack information on dynamic effects, but even worse, the archived hysteretic b_2 measurements, especially at low current include an unknown amount of drift because they were taken at constant current in the magnets.

Table 2 lists the average hysteretic b_2 up the ramp of all Tevatron dipoles currently installed as derived from the magnetic measurement archive at the currents during which the pre-installation measurements were made. The statistical histograms for the ~774 currently installed magnets representing each of these data points are given in appendix 5. Note that the archive magnetic measurement were obtained at ~4.6 K, while the operating temperature in the Tevatron today is 4.0 K. A 0.6 K difference in temperature corresponds to a ~8% difference in hysteretic width (which corresponds to ~1 unit of b_2 at injection). The data in the table were neither corrected for the (unknown) drifts, nor for the temperature difference.

Figure 11 shows a comparison of archived and some recent magnet-based b_2 measurements as a function of current. The graph in Figure 11 clearly shows the discrepancy between the hysteretic b_2 measured in some magnets recently and that predicted on the basis of the Tevatron magnetic measurement archive. Besides the obvious effect of drift at the 660 A and 1 kA points, the plot also shows the large variations in hysteretic width that is to be expected from the large σ associated with each point in Table 2. Also to be taken into account is the larger magnet operating temperature on which the all Tevatron average data are based, which was not corrected for in Figure 11. The variations of geometric b_2 of the single magnets in the figure were removed by replacing it with what we believe is the all Tevatron average geometric b_2. The all Tevatron average geometric is not known exactly and was calculated with the following approach: the all Tevatron average b_2 at ~4 kA, according to Table 2 is 0.83 units. To this we added 0.4 units, which is the average half-width of the hysteretic loop at the same current of all the recently measured magnets. This gives 1.23 units (see dashed line in

plot). (This derivation is discussed further in note [8]). Given the large variation in hysteretic b_2 on the ramp between different magnets and the uncertainties associated with the all Tevatron average due to the drift effects, the comparison of magnet-test-based and beam-based all Tevatron average b_2 can only be approximate.

Table 2: Average up-ramp hysteretic b_2 of all Tevatron dipoles installed, as derived from the archived data obtained from the magnetic measurements performed on all magnets following production. The histograms representing these data are given in appendix 5.

Magnet current (A)	660	1000	2000	3000	4000
Magnet bore field (T)	0.66	1	2	3	4
Beam energy (GeV)	150	227	454	681	908
Average b_2	-4.31	-1.36	0.72	0.87	0.83
b_2 sigma	3.25	3.19	3.13	3.09	3.04

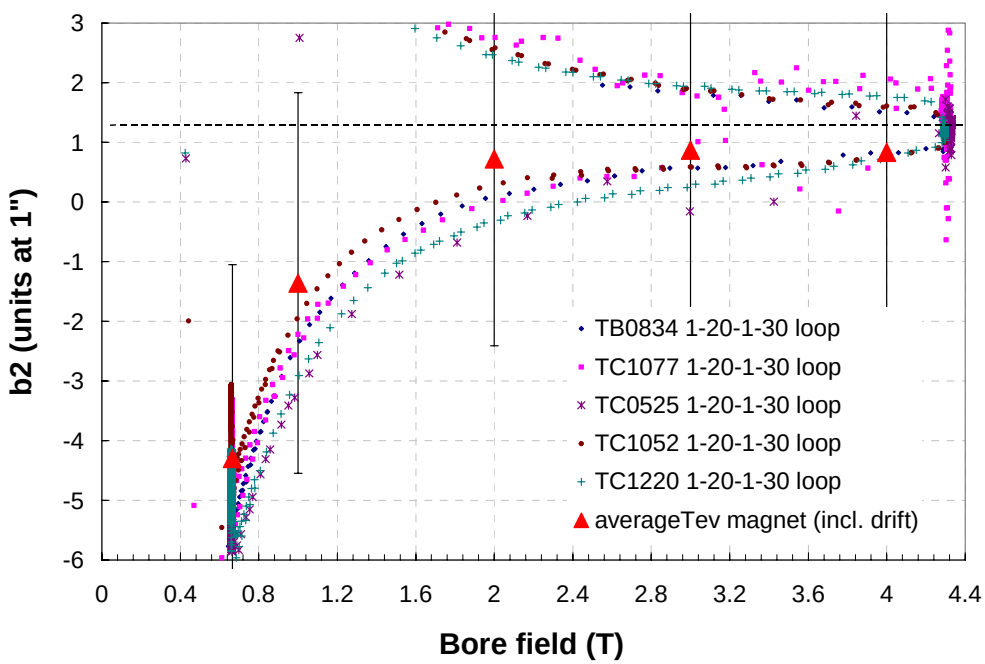

Figure 11: Comparison of archive (average of all installed Tevatron dipoles) and recent hysteretic b_2 measurements in a few Tevatron dipole magnets. The recent magnetic measurements were converted to 4 K, if necessary. The archive data, which were recorded at ~4.6 K were not corrected for the temperature (nor for the drift). The error bars in the archive data correspond to one σ of the Gauss distribution with which all 770 magnet results were fitted. The recent magnet *b2* data were obtained in the magnet body and therefore reflected the typical ~14 units of geometric body b_2, which had to be removed and replaced by the average Tevatron dipole geometric. The all Tevatron average geometric is not known exactly, but was assumed to be 1.23 units (see text for more details)

Figure 12 shows the results of magnetic and beam-based b_2 measurements up the ramp combined. The b_2 data from the magnetic measurements were corrected for the geometric to agree with the average Tevatron geometric as discussed above. The recent magnetic measurement data were also converted to 4 K, if necessary, since this is the average temperature the Tevatron dipoles today, [9]. The temperature conversion consisted in scaling the entire loop with a factor 1.13 per K. Besides the two beam-based measurements and recent magnet test results, the plot also contains the reconstructed average hysteretic loop using the archive data from Table 2. The archive magnetic measurement data were not temperature corrected (they were originally obtained at 4.6 K). The error-bars added to the points of the reconstructed hysteresis represent the standard deviation of the measurement result distributions for the entire magnet population as given in Table 2. The five magnets shown in Figure 12 are indeed within this $\pm 1\sigma$ bracket. Also of interest is that they fall into two distinct classes of magnets, consistent with the two classes of Tevatron magnets in terms of their b_2 magnetization loop widths, [8]. Single magnet measurements are precise to less than 0.1 (magnetic) units. The precision of the beam based measurements is difficult to assess. Also note that the beam-based measurements show strongly different drift amplitudes as a result of the strongly different dwell time at injection (171 min vs. 20 min).

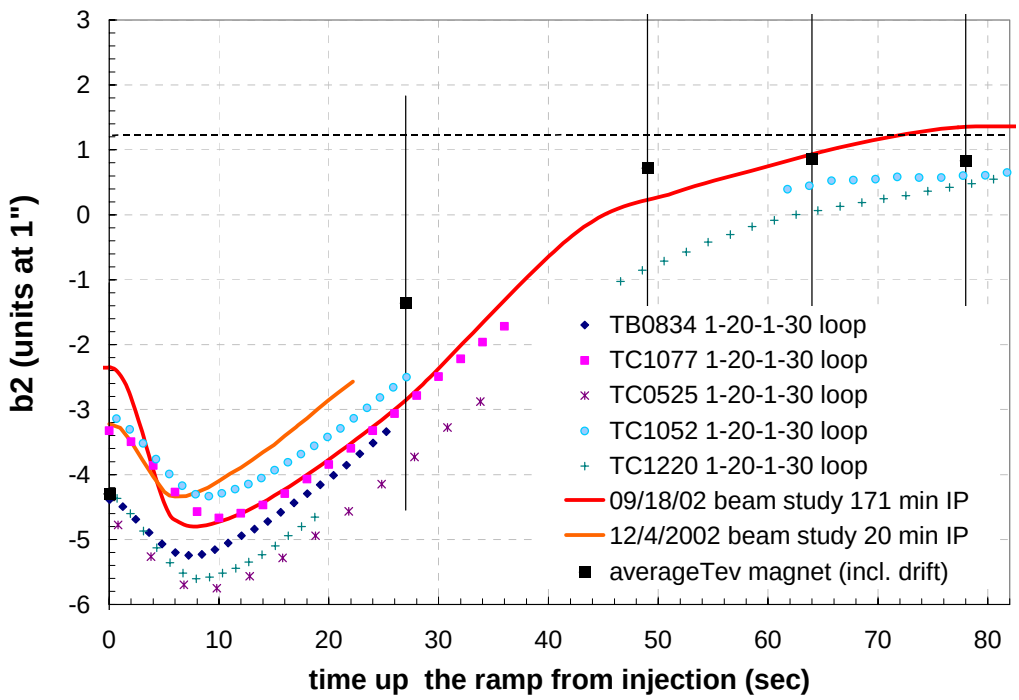

Figure 12: Comparison of beam- and magnet-based b_2 measurements. The recently measured hysteretic loops were converted, if necessary, to the Tevatron operating temperature of 4 K. These magnetic measurements were also offset corrected such as to agree with what we believe is the average geometric b_2 in the Tevatron (~1.23 units). The average Tevatron points are obtained from a reconstruction from the archive magnetic measurement data (error-bars represent 1 σ) in Table 2 and neither temperature nor drift effects were corrected for. The beam-based data are from [7,10]. Note that with the exception of the Sept. 18th beam study result all measurements are for a 1-20-1min pre-cycle and 30 min injection porch.

Figure 13 shows the results of beam-based measurements of the snapback in the Tevatron obtained on 08/10/2004. The chromaticity measurements on the ramp were made after a 1 hr flat-top, 5 min back-porch pre-cycle and a 1 hr dwell at injection. In fact the plot shows two interpretations of the same data, with different hysteretic and geometric b_2 baselines removed from the data. In one case the b_2 baseline with ~-4.5 units (at 150 GeV) was applied, in the other case the b_2 baseline with ~-4.75 units (at 150 GeV). The latter approach is correct if the small jump found in the ramping state study of 04/27/2004 (see Figure 10 for instance) is to be interpreted as a snapback following the unexpected fast drift.

Also to be noted is that the current Tevatron b_2 snapback fit uses a fixed snapback duration of 6 secs, which is clearly shorter than the snapback duration observed in these data. A discrepancy of the order of 0.3 b_2 units (~10 units of chromaticity) would appear toward the end of the snapback between the current fit and the shown data.

We conclude that this comparison of average Tevatron magnet b_2's as derived from beam studies and the magnet-measurement-archive confirm some of the dynamic b_2 characteristics found in dedicated magnetic measurements on a small number of magnets. Among them is the variation of the snapback time with varying drift amplitude. These results, however, are to be interpreted with caution. The comparison of the beam-based b_2 measurement and the re-constructed average Tevatron dipole b_2 from magnetic measurements is made difficult by the measurement accuracy of the beam-based measurement, and, even more importantly the result of an unknown amount of drift that occurred during the production magnetic measurements. We have done what we could to reduce this uncertainty and arrived at the conclusion that the b_2 measured in the Tevatron is consistent with the expectation on the basis of our knowledge of the magnets.

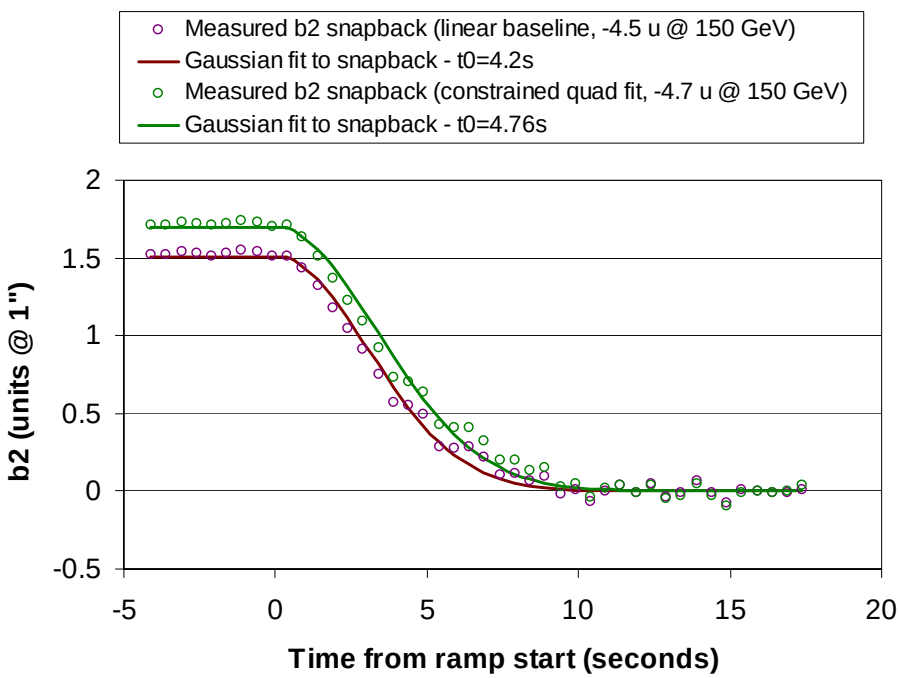

Figure 13: Beam based derived b_2 snapback after a 20 min and a 120 min injection dwell (Dec 4th 2002 beam study data). Also shown are the Tevatron snapback fits. The data are baseline corrected (the growth of hysteretic b_2 during the snapback was subtracted).

6) Conclusions and Recommendations

The comparison of beam-based b_2 measurements and magnet measurements was used to verify how well the b_2 in the Tevatron is understood. One major question that we attempted to answer is whether our understanding of magnet b_2 gained from the study of archived b_2 measurements and recent measurements in select magnets is consistent with the b_2 found in the Tevatron. We believe that the answer is affirmative, albeit within a certain margin of error. The uncertainty is related to the fact that both sets of data are compromised to a certain extent: -1- the archive data suffer from drift effects that were not recognized as such and –2- it is impossible to predict the Tevatron behavior on the basis of data, even if of high quality, obtained on a small sample of magnets, such as was done recently. The discrepancy between a single magnet and the current Tevatron b_2 decay and snapback correction algorithm can be as large as ~0.5 b_2 units, given the large spread of the amplitude of dynamic as well as hysteretic b_2 in Tevatron dipole magnets. Beam-based b_2 data, which provide insight into the average Tevatron magnet, also come with a non-negligible uncertainty. If we can successfully predict the Tevatron chromaticity on the basis of our knowledge of the Tevatron magnets, we can, of course, also improve the feed-forward b_2 correction scheme used in the Tevatron.

We believe that despite the caveats listed above, we were able to reduce the discrepancies between the predicted and measured b_2 sufficiently to confidently develop proposals for improvements of the b_2 correction scheme in the Tevatron. For instance, we found strong evidence that some of the main characteristics of dynamic b_2 effects that were found and investigated in depth in off-line magnetic measurements, such as the dependence of the snapback duration on the drift amplitude, were also present in the Tevatron. We also think that the geometric and hysteretic b_2 properties of the Tevatron dipoles are consistent with that predicted on the basis of the magnet measurements.

Although our work indicates that the current Tevatron b_2 correction works reasonably well, we found room for improvement. In particular there are three aspects of the current Tevatron b_2 correction, which can lead to significant improvements of the quality of the drift and snapback correction in the Tevatron. These improvements should also translate into an increase in Tevatron luminosity as a result of the reduction of beam-loss on the ramp as well as time-savings during shot setup. Our proposed improvements of the Tevatron b_2 correction scheme are:

- Fix (and extend) the back-porch duration in the pre-cycle;
- Eliminate the beamless pre-cycle in most cases, change its parameters in the remaining cases;
- Improve the functional shape of the drift and snapback algorithm;

-1- The off-line magnetic measurements have shown that the back-porch time is the pre-cycle parameter with the strongest impact on the b_2 drift and snapback characteristics in Tevatron magnets. In the current Tevatron shot set-up procedure the time on the back-porch is variable since it requires some manual machine adjustments by the operators. We propose that the back-porch time be fixed in the Tevatron, such as to reduce the shot-

to-shot variability in the dynamic effects. This will be beneficial to the Tevatron in spite of the fact that the Tevatron dynamic b_2 correction algorithm tracks the change of the back-porch time parameter. There are, however, several reasons why the quality of the currently used multi-parameter fit for the dynamic b_2 correction in the Tevatron is poor. First, the algorithm's dependence on flat-top and back-porch dwell-time was derived on the basis of data measured in only one magnet, and the parameters of the multi-parameter fit were not independently varied in a wider range such as to produce a good quality fit. Second, the pre-cycle flat-top energy and the magnet temperature in the magnet measurement was different from the Tevatron. Finally, as discussed in appendix 3, some of the fit parameters were changed during initial implementation of the fit in the Tevatron, thereby changing the functional dependences in the fit. Therefore, with a fixed back-porch time, even in the absence of the "perfect" b_2 correction algorithm, a permanent improvement of the correction should be obtainable with some existing (or a new, see below) fit and modest beam-based adjustments.

Furthermore, as shown in Figure 6, the drift amplitude decreases with back-porch time. Therefore, in order to decrease as much as possible the magnitude of possible errors in the b_2 correction, we propose to also extend the back-porch duration to >5 min, especially of this can be done without a net increase of the total shot setup time.

Also, at the end of the back-porch dwell (now typically 1.5 min), the TCHROM module is loaded to calculate (among other things) the parameters of the drift and snapback fit during the subsequent injection porch. This operation takes typically 20 secs during which the Tevatron is still at the back-porch. The back-porch time measurement currently does not take this effect into account, therefore introducing a 20 sec error in the calculation of the back-porch-time. Such an error produces a ~0.1 unit difference in the current b_2 correction algorithm.

-2- The current collider shot set-up ramp pre-cycle, consists of a ramp to collision energy, followed by a 20 min "dry-squeeze" (=activation of the low beta optics) and a ramp down to injection. The full pre-ramp cycle takes approximately 45 min. The beam-less pre-cycle serves the purpose of bringing all Tevatron main magnets into a reproducible magnetic state given the hysteretic and dynamic effects in their magnetic field characteristics. In the case of a quench, for instance, there are different ramp and temperature histories within the magnet population and the pre-cycle is needed. In certain conditions, however, it is possible to eliminate the pre-cycle and reduce the shot set-up time, therefore increasing the integrated luminosity. The average luminosity lifetime in the Tevatron collider run II thus far is ~16 hrs. Therefore the gain in integrated luminosity that can be generated by eliminating the 45 min pre-cycle can be estimated to be (0.75hrs/16.75hrs)=4.4%. The pre-cycle can only be eliminated when a store was aborted intentionally, however. Table 7 in appendix 6 contains a recent survey of run II store termination scenarios. This table indicates that about two thirds of the stores in the Tevatron are terminated intentionally, thus leading to a total gain in integrated luminosity of ~3%. Obviously the pre-cycle cannot be eliminated when a magnet quench occurred, since the quenched magnet(s) will have very different dynamic effect characteristics that the rest of the ring. One or several pre-cycles have to be applied in order to erase these

differences between the quenched and non-quenched magnets. As shown in Table 7 only three percent of the stores are actually terminated due to magnet quenches. Other store end scenarios that are incompatible with the pre-cycle elimination are magnet failures and cryogenic- and quench protection system failures. All these categories together (including quenches) represent ~14% of all stores in the collider run II according to Table 7.

The elimination of the beam-less pre-cycle will result in a condition in which the preceding shot essentially becomes the pre-cycle of the following shot. That introduces two issues. First the flat-top duration of the pre-cycle can become very long (24 hrs or more). Second, the injection time for the previous shot determines the duration of the so-called front-porch of the pre-cycle and thus the front-porch becomes a variable parameter. Regarding the former we now know that the dynamic b_2 drift and snapback in the Tevatron main dipole increases with the duration of the pre-cycle flat-top duration until a saturation is reached, typically after ~40 min. The increase of the drift amplitude that the elimination of the pre-cycle would entail is not desired. If, as discussed in 1), the back-porch is to be increased at the same time, a net reduction of the drift amplitude with respect to today by ~10% is nevertheless achievable. The saturation of the drift amplitude for flat-tops longer than ~40 mins is a very positive feature, since it results in a reproducible drift and snapback behavior from shot-to-shot (in conjunction, of course, with a fixed back-porch duration), facilitating the b_2 correction. Regarding the latter, a series of measurements was conducted in TB0834 ([8]) to investigate the effect of the front-porch duration on dynamic effects. No noticeable effect was found, leading us to the conclusion that the variable front-porch does not need to be addressed in the b_2 correction.

In the cases, in which the Tevatron stores are not ended intentionally and in which the temperature or ramp sequence is abnormal in some or all magnets a beam-less pre-cycle needs to be performed. We propose, however, to use only one pre-cycle with a ~40 min flat-top instead of the six fast pre-cycles (1 min back-porch dwell, 1 min flat-top, 1 min front-porch dwell) currently applied in the Tevatron operational procedure. In fact we have shown in dedicated measurements that the sequence of six fast pre-cycles results in a less reproducible state than the single pre-cycle with the long flat-top. Figure 14 shows the snapbacks measured in magnet TB1055 after 30 min at injection following six fast pre-cycles as compared to that following a single pre-cycle of varying flat-top duration (and 1 min back-porch). The plot clearly shows that the drift amplitude following the six pre-cycles is not at the saturation value. This is not necessarily a bad condition, but could very well mean that the “memory” of the magnets is not entirely erased. Since the pre-cycles serve to do exactly that, we think it is a safer approach to replace the six fast pre-cycles by one long flat-top (t>40 min) pre-cycle after which the saturation is guaranteed.

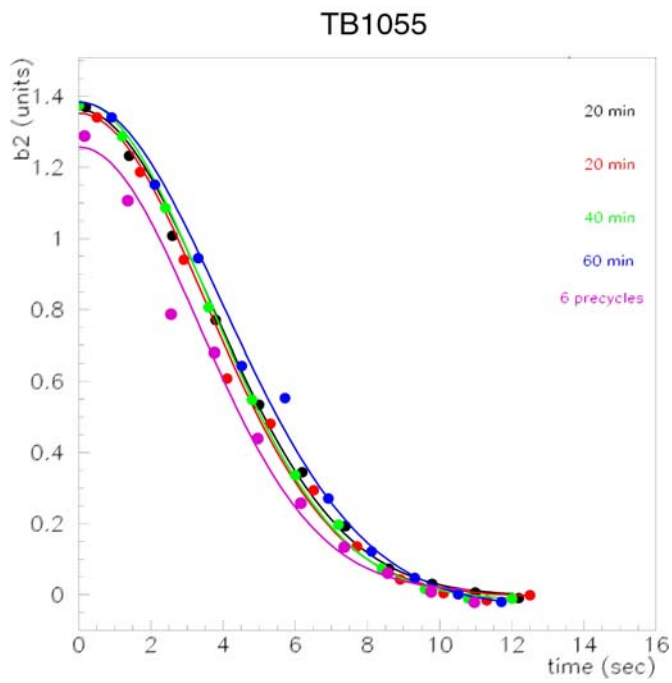

Figure 14: Measured snapbacks in TB1055 following 6 fast pre-cycles (1 min front-porch, 1 min flat-top, 1 min back-porch) as currently performed in the Tevatron, compared to the snapbacks measured following one pre-cycle with varying flat-top duration (1 min front-porch, 1 min back-porch). This graph shows that the drift amplitude in the case of 6 pre-cycles is below saturation.

This change also reduces the thermal load on the Tevatron cryo-system and therefore reduces the risk of temperature variations following the multiple ramps.

-3- The magnet and beam based measurements discussed in chapters 3-5 indicate that the drift amplitude and snapback duration are underestimated in the Tevatron b_2 correction algorithm. Figure 4 gives a good illustration of the issues at hand. Furthermore, as shown for instance in Figure 15, the functional form of the drift and snapback fit in the Tevatron appears to differ from that found from fits of magnetic measurement data. The Tevatron b_2 snapback fit uses a 4th order polynomial (with only even terms) as a function of a single parameter, the snapback duration (equation 4). All snapback measurements performed in 1988, 1992 and 1996 reveal a snapback shape that is suggestive of the polynomial function. We would like to point out, however, that the functional shape of the snapback is altered after removing the hysteretic b_2 baseline (between 150 and ~153 GeV). The fact that the baseline is changing during the snapback was not taken into account in earlier magnet measurement data analysis. The effect should be taken into account, especially since the change of hysteretic b_2 during the snapback is in principle already corrected for with the T:SF and T:SD correction circuits. Furthermore, if plotted as a function of current (or magnetic field in the bore), the snapback appears to be fitted best by an exponential function. In the engineering unit "time" the snap-back, which is exponential in magnetic field (or magnet current), becomes Gaussian because the ramp is parabolic in time. A possible implementation of the Gaussian snapback fit is given in (8), where $b_{2,}^{drift}$ is the drift amplitude at the start of

the snapback (as measured or calculated with a drift algorithm) and t is the time from the start of the snapback. Figure 15 shows that the Gaussian function such as in equ. 8 fits the snapback better than the currently used polynomial form (such as in equ. (4)) or an exponential function. The Gaussian fit is also more robust, because, unlike the snapback duration used now as parameter, it is much less sensitive to data noise at the end of the snapback. Note that the snapback time in the polynomial in Figure 15 was chosen to optimize the fit and is actually 10.5 secs as opposed to the 6 secs time constant currently used in the Tevatron. Unlike in the polynomial fit, however, equation (8) has a time constant, $t_{0,sb}$, that depends on the history parameters through the drift amplitude. This ensures that the snapback takes longer, the larger the drift amplitude.

$$b_2^{snap}(t) = b_2^{drift} e^{-\frac{t^2}{\left(t_{0,sb}\left(b_2^{drift}\right)\right)^2}}, \quad b_2^{drift} = b_2^{drift}\left(t_{bp}, t_{ft}, t_{inj}\right) \quad \textit{units at } 1'' \tag{8}$$

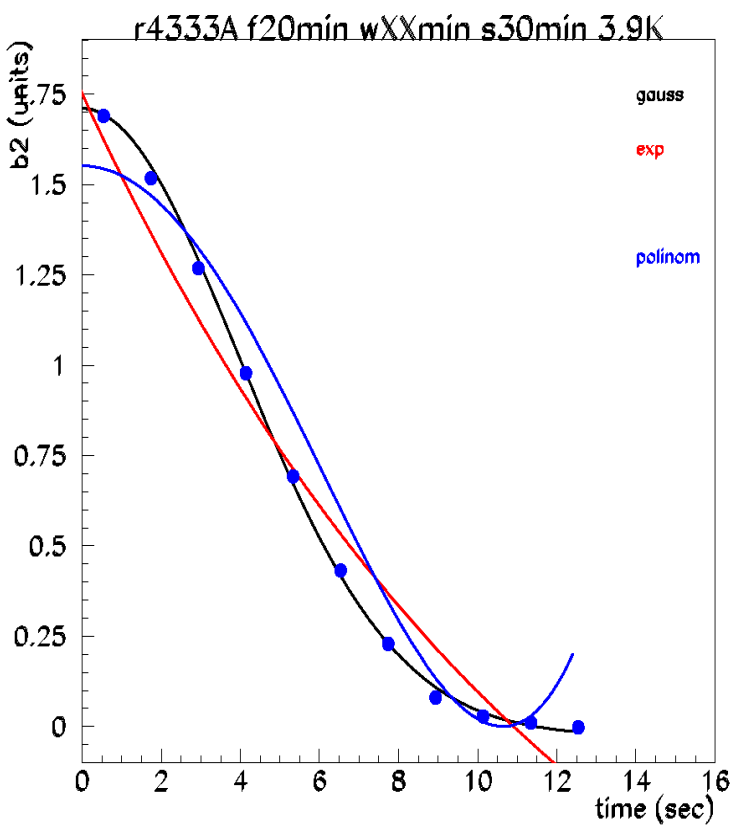

Figure 15: Polynomial and exponential fits of a snapback measured in TC0269 after a 30 min drift following a standard Tevatron pre-cycle (20 min flat-top, 1 min back-porch).

The issues related to the simple logarithmic function (equ. 1) used today to fit b_2 in the Tevatron have been presented in section 2. Among them are a strong disagreement at times <1min when the fit gives a (–1) unit drift and the divergence for $t=0$. These issues

were already recognized in 96, but the simpler fit was nevertheless retained in the Tevatron for practical reasons. The measurements on the magnets, however, are best fitted with an equation of the type (9) over the entire time range. Other fits using sums of several exponential functions have also been shown to fit the data well.

$$b_2^{drift}\left(t_{bp}, t_{ft}, t\right) = m\left(t_{bp}, t_{ft}\right) \times \ln\left(\frac{t + t_{0,d}}{t_{0,d}}\right) \quad units\ at\ 1'' \tag{9}$$

Possible values for the slope m and parameter $t_{0,d}$ are discussed below.

The fit used now in the Tevatron uses a parameter b_{2ini}, which depends on the pre-cycle parameters as in equ. (2). The main purpose of this parameter is to offset the b_2 drift correction at small times by ~(-1) units such as to allow agreement of the fit at $t>1\ min$. We believe that the additional dependence of the offset on the pre-cycle parameters does not reflect the physics of the b_2-drift. In the Tevatron the b_2 value at injection is a well-defined value on the hysteretic b_2 loop of the average dipole, independent of powering history or ramp-rate (at least within a range of ramp-rates typical of the Tevatron's ~70 A/s). Magnetic measurements performed in 1996 as well as today show a variation of this value, referred to as intercept in the b_2 algorithm (equation 2), that is beyond the typical noise of rotating coil measurements. Typical variations are of the order of ±0.1 units. Figure 4, for instance, which shows drift and snapback in eight magnets after removal of the hysteretic and geometric, reveals even larger variations of the starting point of the drift in some magnets. We believe that these changes of b_2 during the dwell at injection or the pre-cycle are related to the so-called longitudinal pattern, discussed briefly in chapter 1. The pattern is a sinusoidal variation in all allowed multipoles (B_0, b_2,..) of the magnet bore-field along the magnet, with an amplitude of several units and with a periodicity given by the cable twist pitch (~2.5 inches in the Tevatron dipoles). If the length of the rotating coil probes, with which the magnetic measurements are obtained, is not an integer multiple of the period of the pattern, the pattern does not integrate to zero and some residual b_2 is picked up. The pattern is caused by the same current imbalances in the coils that cause the drift effects. Therefore its amplitude is powering history dependent. We therefore believe that the history dependence of b_{2ini} is an artifact of the magnetic measurements probes not being an integer number of periods of the periodic field pattern. The order of magnitude of the effect is consistent with the pattern amplitudes measured recently in some Tevatron dipoles, [8]. The beam is believed to integrate over the pattern, such that pattern effects should be irrelevant for the Tevatron. Therefore a variation of b_{2ini} with pre-cycle parameters should not be implemented in the Tevatron chromaticity correction, such as it is currently done (equation 2). The parameter b_{2ini}'s main purpose, however, namely to off-set the correction algorithm by ~(-1) unit, should be retained. Figure 4, however, possibly also includes evidence of the ~0.2 units of fast drift discussed in chapter 5. The fast drift effects can easily be taken into account in equ. (9) by adding ~0.2 units (and thus re-introducing a $b_{2,ini}$ factor, albeit smaller and with "physical" meaning).

The possibility of an improvement of the b_2 correction algorithm in the Tevatron raises the question whether it should be a multi-parameter fit that is able to adapt to changes in the pre-cycle parameters or if it should be simple and applicable only to one particular type of pre-cycle. As discussed in the previous chapters, recent magnetic measurements on several Tevatron dipoles indicate that the currently used multi-parameter algorithm does not fit the functional dependences of drift and snapback on pre-cycle parameters with sufficient precision. The data obtained in the recent magnetic measurement campaign could be used to design an improved multi-parameter fit. Such a fit would be restricted to the effects of back-porch and flat-top duration in the pre-cycle since these are the dominant parameters. To obtain a good multi-parameter fit we would need to perform additional measurements in order to obtain drift and snapback measurements in points of the parameter-space further away from the narrow regions currently investigated (which lie close to the current operational points in the Tevatron). Variations of the ramp-speed or the energies of the pre-cycle plateaus (flat-top, front- and back-porch, reset) as well as Tevatron temperature would not be included because the data are simply not available and cannot be obtained in a realistic time-frame. It is also unlikely that these parameters will be changed since there appears to be no good reason to do so at this point. We believe, however, that it might not be necessary to provide such a multi-parameter fit. If the above recommendations are implemented – namely the back-porch fixed and the flat-top of the pre-cycle extended beyond saturation – there should be no shot-to-shot variations in the b_2 drift and snapback characteristics of the Tevatron (given of course that the other parameters of the pre-cycle profile also remain unchanged). In this case a simple fit with fixed parameters m, $t_{0,d}$ can be implemented for the drift compensation (equ. 9). As discussed below a recent beam-study was conducted to define these parameters. The snapback time constant $t_{0,sb}$ can be computed from the drift amplitude as obtained with equ. (9), or even better, derived from beam studies.

A recent b_2 study was performed as a first step to implement the 5-min back-porch, long flat-top conditions recommended above. In this beam study the Tevatron was prepared with a 2.7 hrs flat-top and 5 min back-porch pre-cycle. The chromaticity was measured during the drift with an un-coalesced center-orbit protons-only beam. The chromaticity data were converted to the average magnet b_2 in the Tevatron. This was done according to the procedures outlined in chapter 5. More details on the beam study results are given in [12]. Figure 16 shows the comparison of the b_2 derived from the measured chromaticity together with the b_2 predicted for similar conditions with the current Tevatron b_2 drift algorithm. The algorithm predicts the measured b_2 behavior reasonably well. It overestimates the drift at t<30 min and over-estimates the drift at t>30 min, causing the chromaticity to first increase by several units and then to decrease. The measured chromaticity on the injection porch varies by ~10 units due to the ~0.2 unit mismatch between the correction algorithm b_2 and the average Tevatron b_2, [12]. The quality of the current fit is surprisingly good since the algorithm was not intended to be used for very long flat-top.

The plot also contains a drift curve derived from a measurement on Tevatron dipole TB0834. Since it was concluded late in the program that the back-porch time should be increased to reduce the amplitude of the dynamic effects only one magnet was tested

systematically at longer back-porch times. The fit to a measurement result shown is for a 60 min flat-top and 5 min back-porch condition. Since the drift parameters (slope,..etc) saturate at flat-top times longer than ~40 min (see a detailed discussion of this effect in [8]) this measurement is also representative of the 2.7 hr flat-top pre-cycle in the beam study. It is evident from Figure 16 that the fit to the magnetic measurement on TB0834 agrees much less with the measured average Tevatron behavior than the existing algorithm. This is not surprising, since TB0834 is not representative of the average Tevatron magnets. In fact, according to comparisons with ten other magnets shown in Figure 4, TB0834 is the magnet with the smallest drift amplitude of all magnets studied recently. It is noteworthy, however, that the TB0834 drift fit can be made to agree with the average Tevatron b_2 drift through a simple scaling factor (here 1.75). The agreement after scaling is in fact better than the agreement obtained with the current algorithm. The geometric and hysteretic b_2 were removed and replaced by –4.5 units in the TB0834 shown in the plot. This b_2 value is believed to be close to the average hysteretic b_2 of the Tevatron at 150 GeV, as discussed in chapter 4. This procedure was also used for the Tevatron drift algorithm. In both cases this value appears to be a reasonable choice given the close agreement of these data with the chromaticity derived b2 measurement.

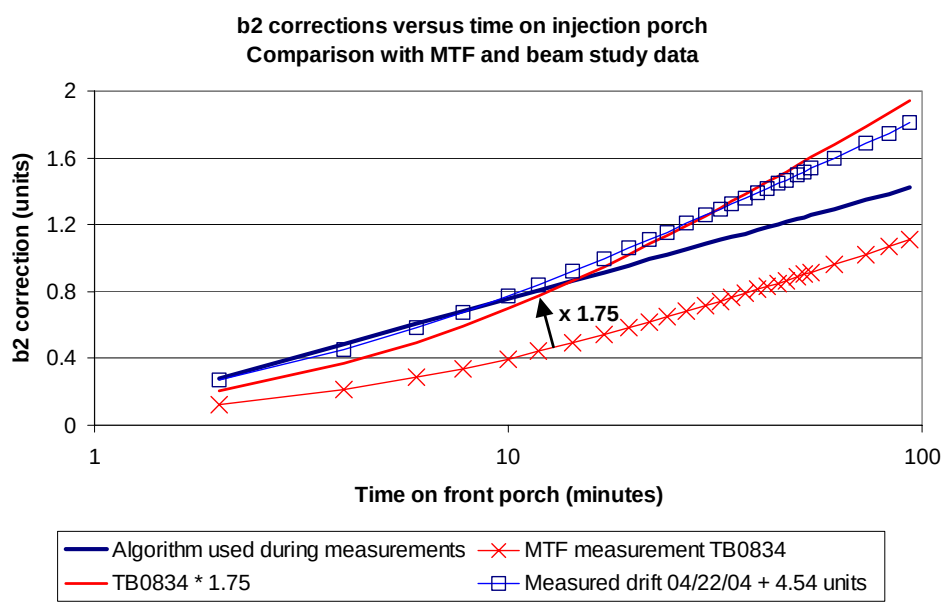

Figure 16: Result of beam based measurement of *b2* on injection porch following a long flat-top and 5 min back-porch.

This beam study therefore indicates that ***m~0.5u*** (1.75 times that of TB0834) and $\boldsymbol{t_{0,d}}$**=170 sec** (as in TB0834) inserted in equ. (9) would be representative of the Tevatron average. Once the drift is known the snapback time constant can be calculated from $b_2^{drift}(t_{inj})$ with:

$$t_{0,sb}\left(b_2^{drift}\left(t_{inj}\right)\right)=\sqrt{\frac{\left(b_2^{drift}\left(t_{inj}\right)-a\right)}{b}} \quad (\text{sec}) \quad \text{, where } \mathbf{a=0.0606} \text{ and } \mathbf{b=0.0682} \qquad (10)$$

APPENDIX 1

The units of sextupole, b_2, can be converted to current in the two sextupole circuits (T:SFB2 and T:SDB2) via the chromaticity relation (at 150 GeV):

$$\begin{pmatrix} \Delta\zeta_x \\ \Delta\zeta_y \end{pmatrix} = \begin{pmatrix} 45 & 8.9 \\ -14.36 & -26.96 \end{pmatrix} \begin{pmatrix} I_{T:SF} \\ I_{T:SD} \end{pmatrix} \qquad (units\ of\ chromaticity) \tag{A1}$$

and the relation between chromaticity and b_2 in the dipoles:

$$\begin{pmatrix} \Delta\xi_x \\ \Delta\xi_y \end{pmatrix} = \begin{pmatrix} +26.22 \\ -23.92 \end{pmatrix} b_2 \quad (units\ of\ chromaticity) \tag{A2}$$

The matrix elements $M_{i,j}$ in (A1) were calculated from (A3), where the index i stands for x,y and the index j for SF and SD. The lattice functions in both circuits are given in Table 3 and were obtained with the MAD program for a model of the Tevatron lattice.

$$M_{i,j} = \frac{1}{4\pi} \times 88 \times \langle \beta_i D_i \rangle_j \frac{449\,T/m}{(500\,Tm)_{dip} \times 50A} = \frac{1}{4\pi} \times 88 \times \langle \beta_i D_i \rangle_j \times 0.01795 \left(\frac{units}{A} \right) \tag{A3}$$

Table 3: Sextupole corrector characteristics (calculated with Tevatron lattice model in MAD).

Circuit	Number of elements	Average β_x (m)	Average β_y (m)	Average D_x (m)	Average β_x*D_x (m^2)	Average β_y*D_x (m^2)
T:SF	88	93.81	30.09	3.810	358.7	115.8
T:SD	88	30.30	93.29	2.301	70.84	214.6

The coefficients in (A2) can be calculated similarly (on the basis of MAD model data) from (A4):

$$\begin{aligned} \xi_x &= \frac{1}{4\pi} \sum \beta_x K_2 L D_x = \frac{1}{4\pi} N_{dip} \langle \beta_x D_x \rangle L_{dip} K_2 = \frac{1}{4\pi} N_{dip} \langle \beta_x D_x \rangle L_{dip} \frac{2B_0 b_2 10^{-4}}{B\rho r_0^2} = \\ &= \frac{774 \cdot 170 \cdot 6.12 \cdot 2 \cdot 0.66 \cdot b_2 10^{-4}}{4\pi \cdot 500 \cdot (0.0254)^2} = 26.22 \cdot b_2 \\ \xi_y &= -23.92 \cdot b_2 \end{aligned} \tag{A4}$$

As can be seen in (A4) the sextupole strength K_2 is defined as $(2B_0 b_2 10^{-4})/(B\rho r_0^2)$. Inverting the matrix in (A1, A2) and using (A4) gives equation (A5) for the currents in the correctors (at 150 GeV).

$$\begin{pmatrix} I_{T:SF} \\ I_{T:SD} \end{pmatrix} = \frac{1}{1085}\begin{pmatrix} -26.96 & -8.9 \\ 14.36 & 45 \end{pmatrix}\begin{pmatrix} +26.22 \\ -23.92 \end{pmatrix} b_2(units) \qquad (A) \tag{A5}$$

Equation (A5) can be made explicit to give the linear current-b_2 relations:

$$I_{T:SFB2}(t) = -0.454\, b_2(units) \quad (A) \tag{A6}$$

$$I_{T:SDB2}(t) = -0.646\, b_2(units) \quad (A) \tag{A7}$$

The constants quoted in (A6) and (A7) are the calculated values for the Tevatron. They do not match exactly those measured in the Tevatron (see equations (5) & (6) in the text). For further discussion consult reference [7].

APPENDIX 2

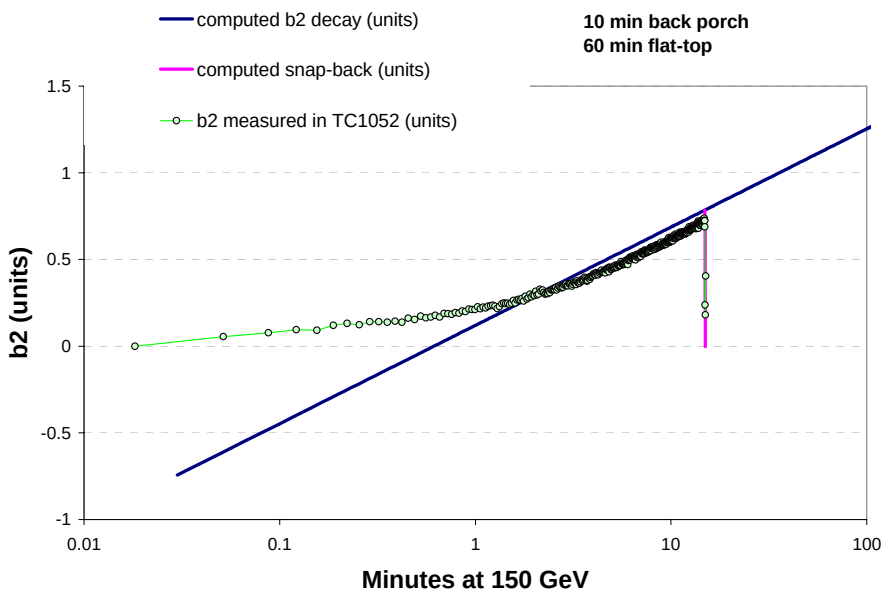

Figure 17: Sextupole decay in TC1052 for 10 min back-porch and 60 min flat-top conditions as compared to the calculated sextupole (equ (1)-(4). The b_2 is given in units at 25.4 mm.

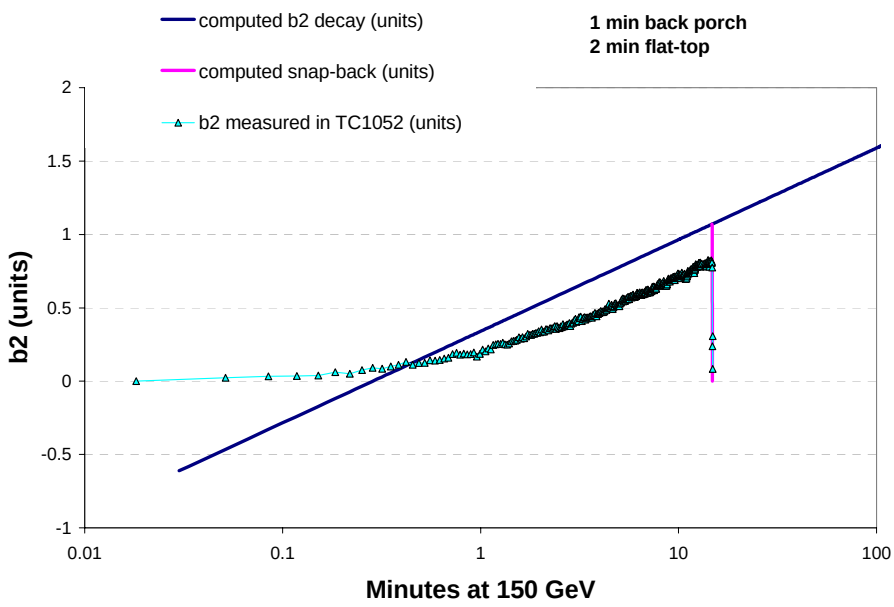

Figure 18: Sextupole decay in TC1052 for 1 min back-porch and 2 min flat-top conditions as compared to the calculated sextupole (equ (1)-(4). The b_2 is given in units at 25.4 mm.

APPENDIX 3

The algorithm currently used for the b_2-decay and snapback correction is described in detail in chapter 2 (and was recently documented thoroughly in [5]). The following presents a new analysis of the 1996 magnetic measurements performed on the Tevatron dipole model TC1052. The original data analysis, which led to the algorithm presented in chapter 2, was published in [4]. This work is therefore a repetition of the work presented there. The goal of this exercise is to determine how far the algorithm currently used in the Tevatron has evolved from the initial one. It is believed that this discrepancy is somehow indicative of the difference between the average Tevatron dipole magnet and TC1052. It also reflects differences in key operating parameters between the test of dipole 1052 the Tevatron, such as for example in the pre-cycle conditions and the temperature. The following presents the recently obtained fits to the TC1052 data.

The chosen fitting procedure consisted in using a least-square method to obtain the parameters, b_0 (intercept) and m (slope), of the function $b_0+m\ln(t)$ that fits best the decay data in the range 150sec-15min. Also, the b_2 at 1 sec was subtracted from the intercept (the additive constant in the logarithmic fit) to eliminate the geometric and hysteretic sextupole, which are not of interest for the drift and snapback fits. Figure 19 shows an example of the fitting procedure. The slope and intercept parameters were read directly from the trend-lines in the plot. Figure 21 and Figure 20 show the slopes and intercepts found from the fits for cases of varying flat-top for 1 and 10 min back-porch time. Table 4 and Table 5 summarize the slopes and intercepts extracted from the fits of the decays for different back-porch and flat-top times.

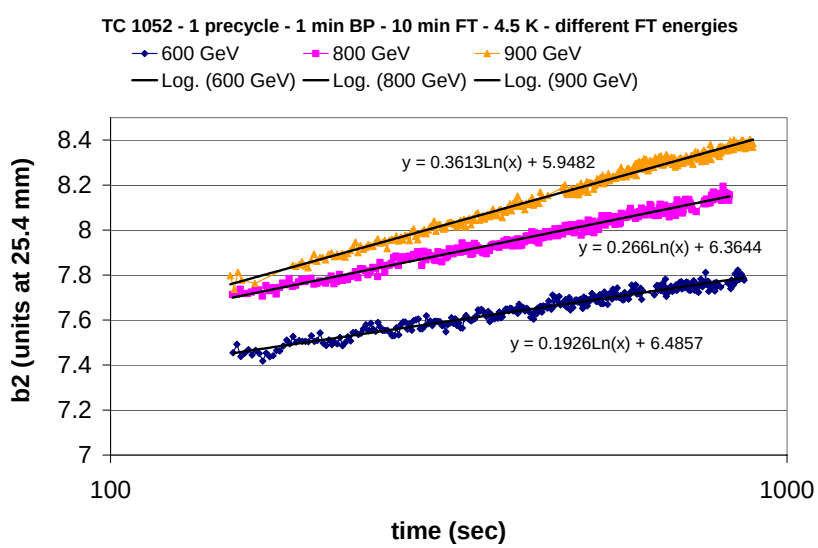

Figure 19: Example of fitting procedure for TC1052 b_2 decay data. The data shown represent cases with varying flat-top current in the pre-cycle. The flat-top condition is indicated in terms of the beam energy. The flat-top duration was 10 min, the back-porch time 1 min. The graph shows the b_2 as a function of time on the injection porch (as explained in the text the first 150 sec were removed from the data prior to fitting).

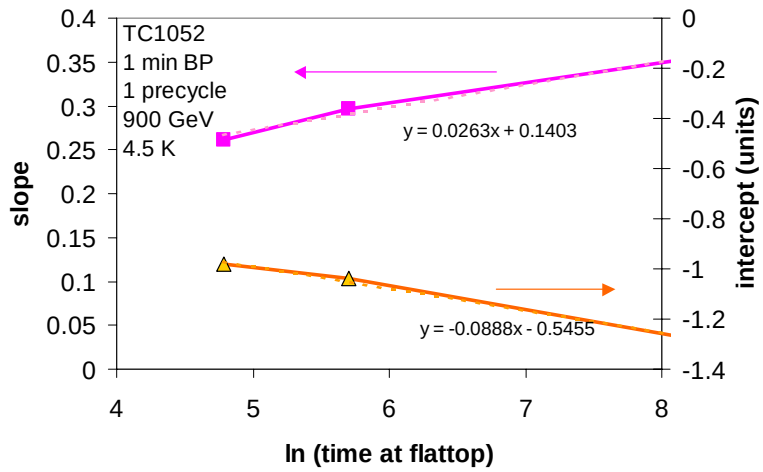

Figure 20: Slope and intercept (in units at 25.4 mm) parameterization in flat-top time (in seconds) of TC1052 data (back-porch time is 1 min).

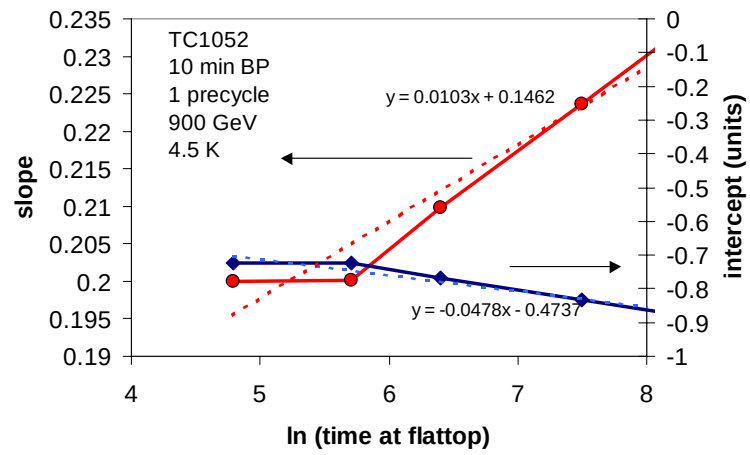

Figure 21: Slope and intercept (in units at 25.4 mm) parameterization in flat-top time (in seconds) of TC1052 data (back-porch time is 10 min).

Table 4: Slope data for TC1052 (4.5 K, 1 pre-cycle, 900 GeV flat-top) for different back-porch, t_{ext}, and flat-top, t_{ft}, times (in minutes).

t_{ft}(min) → t_{ext} (min) ↓	2	5	10	30	60
1	0.261	0.297	-	-	0.354
10	0.2	0.2	0.21	0.224	0.233

Table 5: Intercept (in units at 25.4 mm) data for TC1052 (4.5 K, 1 pre-cycle, 900 GeV flat-top) for different back-porch, t_{ext}, and flat-top, t_{ft}, times (in minutes).

t_{ft}(min) → t_{ext} (min) ↓	2	5	10	30	60
1	-0.98	-1.039	-	-	-1.276
10	-0.725	-0.722	-0.769	-0.833	-0.875

The so found intercept and slopes can be parameterized in terms of t_{bp} and t_{ft} such as in (2) and (3). This was done using a minimization algorithm in *PAW*. The obtained constants A-E are listed in Table 6. The discrepancy between the so found parameters at those in Table 1 is small in B-E, but large in A. This results in a more negative b_2 intercept in the 96 data than what is currently used in the Tevatron fit. Although this is not immediately apparent from the data in Table 6, the discrepancy between the current fit ((2)-(3)) and the TC1052 data is most pronounced for small flat-top times. Figure 22 and Figure 23 compare the slopes and intercepts derived from the TC1052 data and as used in the current Tevatron fit. This discrepancy would further increase if the magnet data would be corrected for the difference in flat-top energy between the 96 magnetic measurements (900 GeV) and today's Tevatron collision energy (980 GeV). Figure 24 shows the fit to the measurements taken at varying flat-top energies.

Table 6: Parameters of sextupole decay algorithm (2) and (3) as currently used in the Tevatron and as derived from the 96 measurement on TC1052 with PAW.

Parameter	A	B	C	D	E
As used today	0.04	0.161	0.0277	0.342	0.0208
Fit to TC1052 data	0.206	0.172	0.0539	0.456	0.019

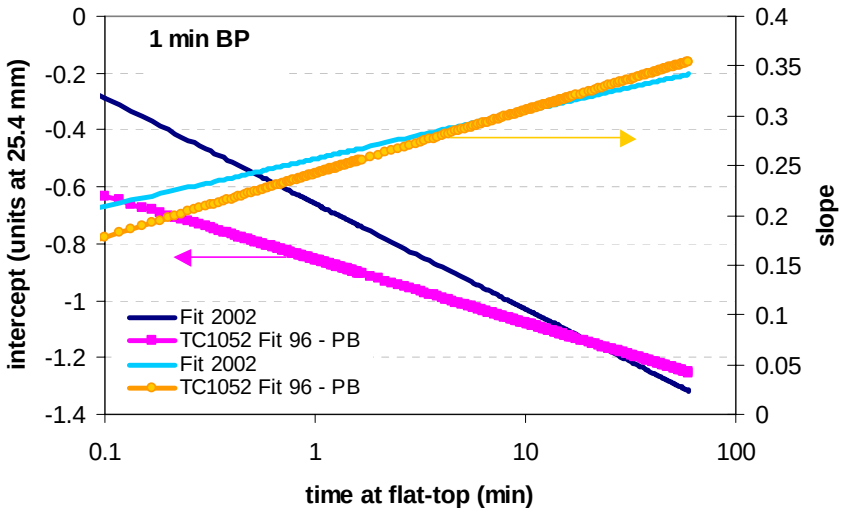

Figure 22: Comparison of slope and intercepts of current Tevatron decay fit and the latest fit to the 96 measurements in TC1052 for different flat-top times. The back-porch time is fixed at 1 min. The measurement conditions were: 1 pre-cycle, 900 GeV flat-top, 4.5 K.

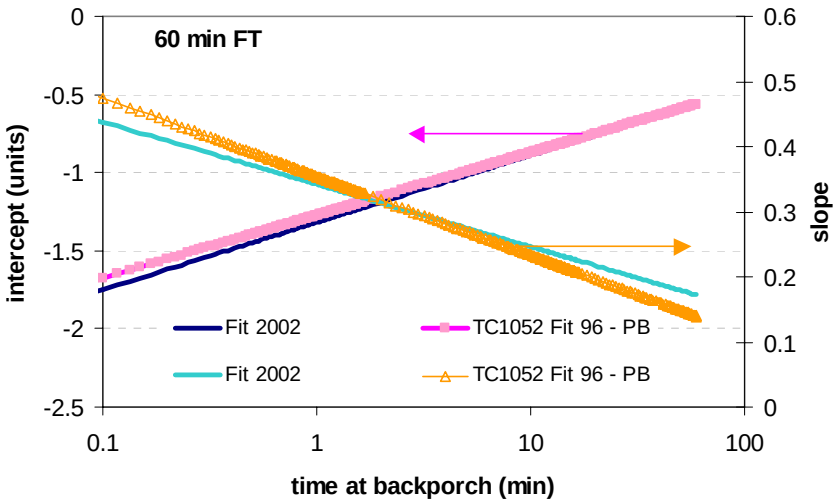

Figure 23: Comparison of slope and intercepts (in units at 25.4 mm) of current Tevatron decay fit and the latest fit to the 96 measurements in TC1052 for different back-porch times. The flat-top time is fixed at 60 min. The measurement conditions were: 1 pre-cycle, 900 GeV flat-top, 4.5 K.

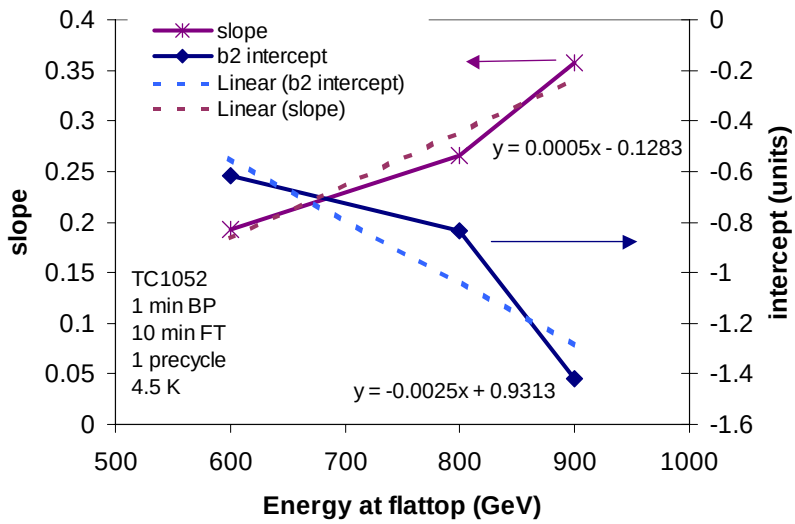

Figure 24: Slope and intercept (in units at 25.4 mm) parameters for TC1052 for a 10 min time at different flat-top energies. A linear fit of the data is shown as well. The measurement conditions were: 1 min back-porch, 1 pre-cycle, and 4.5 K.

APPENDIX 4

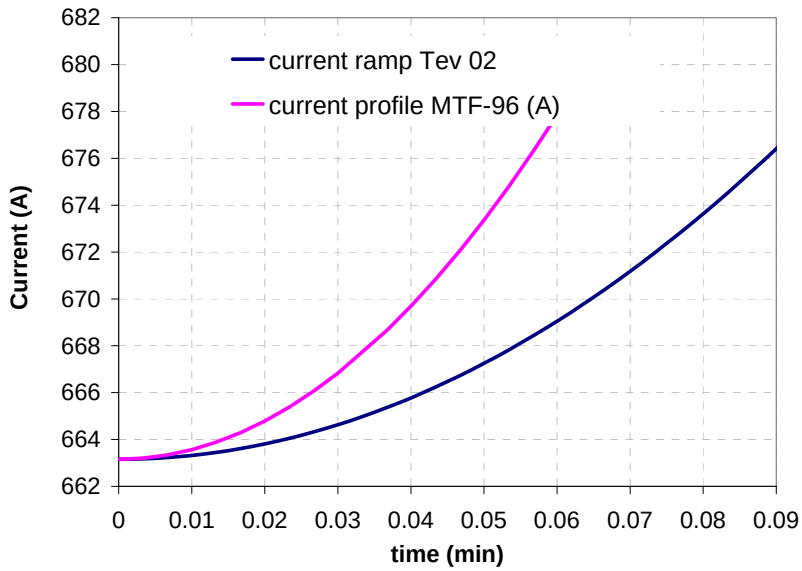

Figure 25: Current profiles for ramp from injection in the Tevatron today and the MTF measurements performed in 1996.

APPENDIX 5

Below are the histograms for the hysteretic b_2 measured in all installed Tevatron dipoles at different currents. The mean and sigma values in Table 2 were derived from these histograms. One open issue is the value of the all Tevatron average of the geometric b_2. The overall Tevatron geometric b_2 can be computed from the up-down branch hysteretic average at 2 kA, which gives 1.47 units. As stated in Table 2 the hysteretic b_2 closest to the flat-top (at 4 kA) is 0.83 units. If the up-down branch average at 2 kA is the geometric, then one would get a hysteretic width of (1.47-0.83)×2, which is larger than the ~0.8 units that are measured in the dozen or so recently tested magnets. It could be that deformations of the loops at higher currents cause this discrepancy. One should note, however, that the geometric b_2 is more or less independent of field in the Tevatron dipoles because iron saturation effects are small and Lorentz-forces are moderate. Most likely this inconsistency is the combined result of high current deformations of the hysteretic loops and differences in the drift amplitude at 2 kA between the up and down ramp measurements. The geometric used in the discussion in chapter 4 of this note was 0.83 + 0.8/2=1.23 units. This result, however, assumes that the 0.8 units, which is the "turn-around-width" of the hysteretic loops in a dozen magnets measured recently is representative of the all Tevatron average loop width at 4 kA.

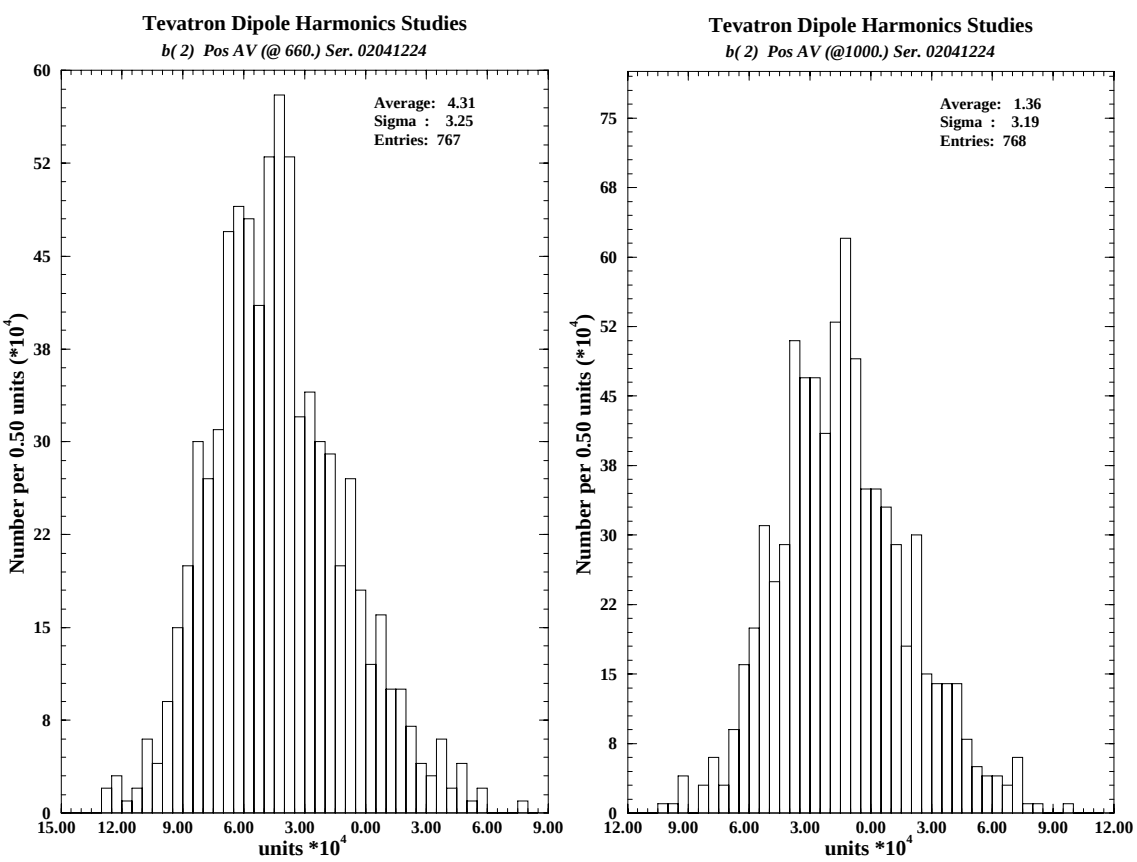

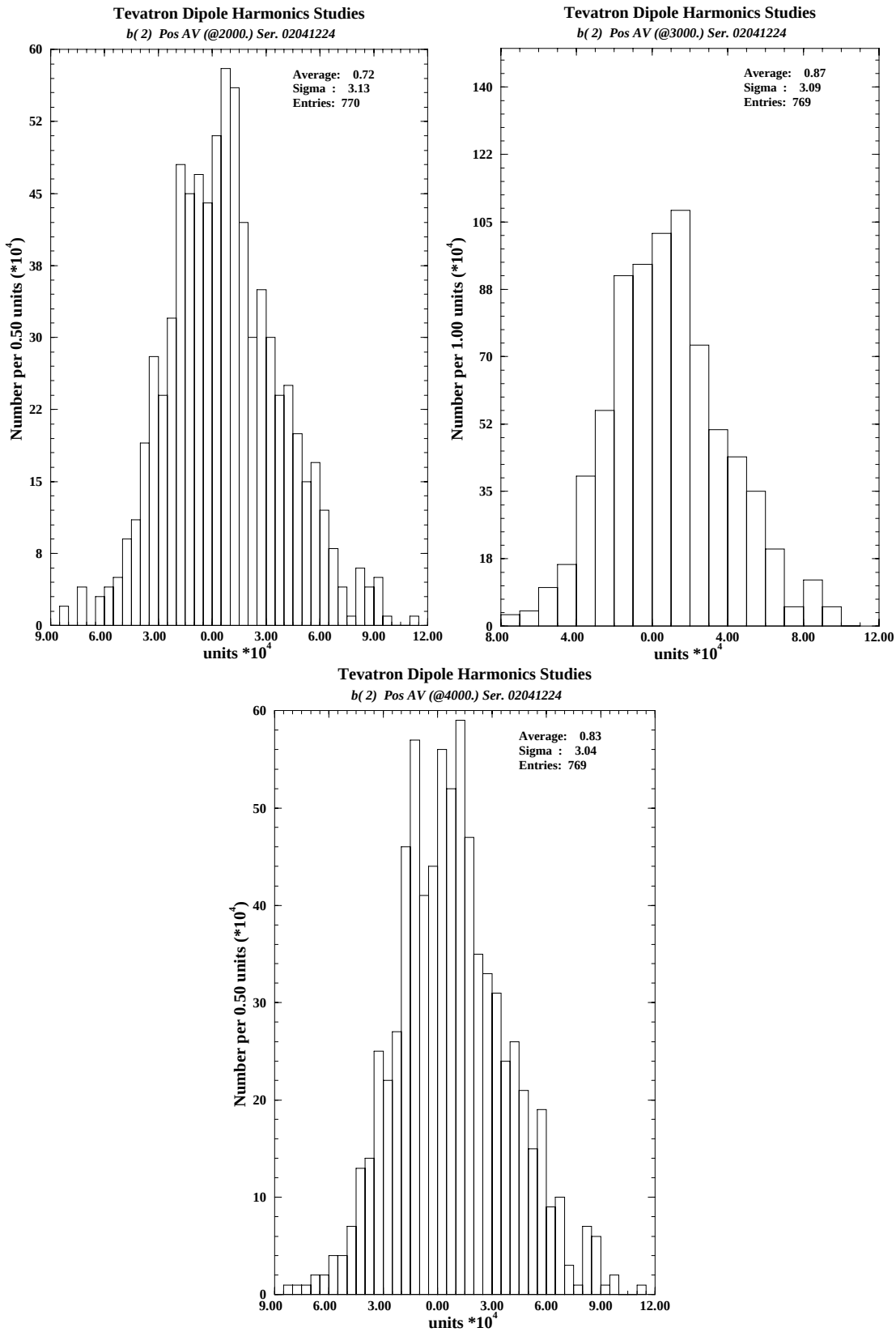

Figure 26: Histograms for hysteretic b2 at 0.66, 1, 2, 3 and 4 kA of all Tevatron dipoles installed.

APPENDIX 6

Table 7: Summary of Tevatron collider run II stores thus far.
Table is courtesy of D. Johnson / Fermilab.

Reason for terminating store	# of stores terminated	Store hours
Intentional	285	5036.48
Controls	8	68.38
Correction Magnet Systems	3	7.21
Cryogenics	22	233.11
Experimental Areas	3	65.76
Glitches/Lightning	17	187.98
Human Error	3	57.78
Instrumentation	0	0.00
Kickers	8	64.61
Low Beta Quadrupoles	6	42.27
Magnet Failure	2	26.55
Miscellaneous	4	25.99
Quench	11	104.36
Quench Protection System	22	175.24
Separators	3	8.31
Tevatron Power Supplies	7	41.99
Tevatron RF	6	39.80
Utilities	0	0.00
Vacuum	1	7.58
Sum	411	6193.4

References

1 D.A. Herrup et al., "*Time Variations of Fields in Superconducting Magnets and their Effects on Accelerators*", Proceedings of the 1988 Applied Superconductivity Conference, IEEE Transactions on Magnetics, Vol. 25, No. 2, 1643-1646, March 1989 (also available as Fermilab Technical Memo TM-1543)

2 P. Bauer et al., *"Tevatron Magnetic Models, Geometric, and Hysteretic Multipoles in the Tevatron Dipole"*, Fermilab, Technical Division, internal note TD-02-040, http://www-td.fnal.gov/info/td_library.html, revision 2, April 2004

3 M. Haverkamp, "*Decay and Snapback in Superconducting Accelerator Magnets*", PhD thesis, Twente University, Netherlands, 2003;

4 G. Annala et al., "*Tevatron Dipole Measurements at MTF*", write-up of 1996 magnetic measurements on magnets TC0504 and TC1052, http://www-bdnew.fnal.gov/tevatron/adcon/magnets.html

5 M. Martens, G. Annala, "*Chromaticity, Tune and Coupling Drift and Snapback Correction Algorithms in the Tevatron*", Fermilab/BD/Tev note Beams-doc-467, Feb. 24th, 2003, direct link: http://beamdocs.fnal.gov/cgi-bin/public/DocDB/ShowDocument?docid=467

6 P. Bauer, *"Historical Review of the Discovery of Dynamic Effects in Tevatron Magnets"*, Fermilab-Technical Division, internal note, TD-03-007, Feb. 2003

7 M. Martens, P. Bauer, D. Still, G. Annala, "*Measurement of the Average B2 Component in the Tevatron Dipole Magnets at the Start of the Energy Ramp*", Fermilab Beams Division, internal note, Beams-Doc-478, March 2003

8 G. Velev et al., "*Measurements of Geometric, Hysteretic and Dynamic Sextupole in Tevatron Dipoles*", Fermilab-Technical Division, internal note TD-04-043, Dec 2004;

9 J. Theilacker, Fermilab/AD, personal communication

10 M. Xiao, Fermilab/AD, personal communication

11 Courtesy of L. Bottura, Cern/LHC/MTA

12 M. Martens et al., "Tevatron Chromaticity and Tune Drift and Snapback Studies Report", Fermilab-Accelerator Division-Tevatron department internal note Beams-doc 1236 (v1.4), Dec 2004;

13 L. Bottura et al., "*A Scaling Law for the Snapback in Superconducting Accelerator Magnets"*, presented at the 2004 Applied Superconductivity Conference, Jacksonville USA, Oct 2004, also available as Fermilab conference memo FNAL-Conf-04-230-TD;